Department of Chemistry
University of Helsinki
Finland

SOFT POLY(*N*-VINYLCAPROLACTAM) NANOPARTICLES IN AQUEOUS DISPERSIONS

Joonas Siirilä

ACADEMIC DISSERTATION

To be presented, with the permission of the Faculty of Science of the University of Helsinki, for public examination in room P674, University building Porthania, on 28 April 2020, at 12 noon.

Helsinki 2020

Supervisor

Professor Heikki Tenhu
Department of Chemistry
University of Helsinki
Finland

Opponent

Professor Dr. Brigitte Voit
Leibniz Institute of Polymer Research Dresden
Germany

Reviewers

Professor Jukka Seppälä
Department of Chemical and Metallurgical Engineering
Aalto University

&

Professor Mauri A. Kostiainen
Associate Professor
School of Chemical Engineering
Aalto University

ISBN 978-951-51-6008-9 (pbk.)
ISBN 978-951-51-6009-6 (PDF)

Unigrafia
Helsinki

ABSTRACT

Soft nanoparticles are attractive materials due to their small size, deformability, and ability to host guest molecules. Possible applications include for example carriers of active ingredients such as drugs, biomolecules, reagents, and catalyst. Soft nanoparticles can also be used to stabilize emulsions and in diagnostic systems.

Poly(*N*-vinylcaprolactam) (PNVCL) is a potential material for the construction of such soft nanoparticles as the polymer is non-toxic and thermoresponsive. The responsiveness allows for facile synthesis of nanoparticles in water and can be utilized in the loading and releasing active compounds from the soft nanoparticles.

From the broad variety of synthesis methods to produce PNVCL particles, selected methods are discussed, utilized and compared in this dissertation.

First, the well-known precipitation polymerization method was used to synthesize colloidal PNVCL gel particles with semibatch method with propargyl acrylate as a comonomer to obtain particles with propargyl moieties on their outer shell. The propargyl groups were later utilized in the functionalization of the gel particles using copper catalysed azide-alkyne cycloaddition.

Functionalization with azide bearing gold nanoparticles yielded particles that shrank in response to temperature, and due to AuNPs, the particles also shrank in response to blue light and to oscillating electric field. Thus, the functionalization of the PNVCL gel particles produced multi-responsive particles.

Propargyl containing PNVCL particles were also functionalized with carbohydrate azides based on either maltose or glucose to obtain particles with biorelevant functions. The accessibility of the carbohydrate groups was evaluated based on protein interaction studies. Interestingly, the carbohydrate functions were accessible at room and body temperatures independently on the swelling degree of the gel particles, swollen versus partly shrunken. This is due to the prencence of the carbohydrates on the outer parts of the gel particles independent of temperature. The morphology and colloidal properties of the carbohydrate functionalized particles were thoroughly investigated and compared to the propargyl functional particles and to particles synthesized without propargyl containing comonomer.

Final part of the dissertation is dedicated to the polymerization induced self-assembly (PISA) of *N*-vinylcaprolactam as the only monomer. The method produces soft PNVCL particles, but these are self-assemblies of PEG-PNVCL block copolymers, not chemically crosslinked gel particles as the ones usually produced using precipitation polymerization. In the PISA reactions performed, control over the molecular mass of the formed polymers was achieved and the polymerizations were made in higher concentration

compared to the concentrations used in the traditional precipitation polymerization method. However, the PISA produced PEG-PNVCL self-assemblies disassembled into dissolved polymer chains upon cooling as the PNVCL block became soluble. Physical crosslinking based on a hydrogen bond donor, salicylic acid, was studied and proved to be effective in preventing the disassembly induced by cooling.

ACKNOWLEDGEMENTS

Work included to this dissertation was conducted in the years from 2014 to 2020 at the department of Chemistry, University of Helsinki. Academy of Finland, the Funding Agency of Innovation (TEKES), Magnus Ehrnrooth Foundation and the University of Helsinki are acknowledged for funding the research.

I am grateful to my supervisor Heikki Tenhu for support and guidance during my studies. I also wish to thank professors Seppälä and Kostiainen for reviewing this dissertation and professor Voit for agreeing to be the opponent. All coauthors of my articles are thanked for their collobaration. Students doing their internship/practice with me are thanked for their enthusiams, work and the inspiration it brought me, especially I thank Sara Miralles, Satu Häkkinen and Luca Guagneli. All the co-workers at the laboratory of polymer chemistry are thanked for the company, help, and for the inspiring atmosphere. Lab engineer Sami-Pekka Hirvonen is thanked for his work, especially in helping me to construct the device to create oscillating electric fields. Vladimir Aseyev is acknowledged for helping me with light scattering. During this time period Sirkka-Liisa Maunu acted as the head of the laboratory and she is my former supervisor, is thanked for providing the possibility to work and for the guidance. Last, I want to thank Fabian Pooch for being my officemate and for the discussions about science, politics and life.

During my PhD studies, I have also lived life and had two children Venla and Urho with my beautiful and kind wife Marjaana. You are the true meaning of my being. I acknowledge you for the motivation and enabling me to pursue interesting challenges. Rest of my family and my friends are also thanked as you make life more enjoyable.

CONTENTS

LIST OF ORIGINAL PUBLICATIONS

This thesis is based on the following publications:

I Siirilä J.; Karesoja M.; Pulkkinen P.; Malho, J.-M.; Tenhu. H. **Soft poly(*N*-vinylcaprolactam) nanogels surface-decorated with AuNPs. Response to temperature, light, and RF-field,** *Europ. Polym. J.* 115, **2019**, 59-69

II Siirilä J.; Hietala S.; Ekholm F. S.; Tenhu H.; **Glucose and Maltose Surface-functionalized Thermoresponsive Poly(*N*-Vinylcaprolactam) Nanogels,** Biomacromolecules, **2020**, 21, 2, 955-96

III Siirilä J.; Häkkinen S. Tenhu H. **The emulsion polymerization induced self-assembly of a thermoreponsive polymer poly(*N*-vinylcaprolactam),** *Polym. Chem.* **2019,** 10, 766-775

The publications are referred to in the text by their roman numerals.

The author`s contribution to the publications:
For the three publications J. Siirilä has drafted the research plan, designed the experiments and conducted most of the synthesis and characterization. However, in paper II the carbohydrate azides were designed, synthesized and analyzed by Filip Ekholm. For all three publications Siirilä wrote the first draft of manuscripts and finalized them with the coauthors.

ABBREVIATIONS

ATR	attenuated total reflection
ATRP	atom transfer radical polymerization
AuNP	gold nanoparticle
BAC	*N,N`*-bis(acryloyl)cystamine
CMC	critical micelle concentration
Con A	concanavalin A
CuAAc	copper-catalyzed azide-alkyne cycloaddition
CTA	chain transfer agent
DCM	dichloromethane
DFM	dimethylformamide
D_h	hydrodynamic diameter
DSC	differential scanning calorimetry
EDTA	ethylenediaminetetraacetic acid
EPR	enhanced permeability and retention
HEPES	2-[4-(2-hydroxyethyl)piperazin-1-yl]ethanesulfonic acid
IR	infrared
IUPAC	International Union of Pure and Applied Chemistry
KPS	potassium persulfate
NMR	nuclear magnetic resonance
MADIX	macromolecular design via the interchange of xanthates
PA	propargyl acrylate
PEG	poly(ethylene glycol)
PISA	polymerization induced self-assembly
PNIPAm	poly(*N*-isopropylacrylamide)
PNVCL	poly(*N*-vinylcaprolactam)
RAFT	reversible addition-fragmentation chain transfer
R_g	radius of gyration
R_h	hydrodynamic radius
RT	room temperature
SAXS	small-angle x-ray scattering
SEC	size exclusion chromatography
SDS	sodium dodecyl sulfate
VPT	volume phase transition
wt%	weight procent

1 INTRODUCTION

1.1 NANOPARTICLES

Nanoparticles[1] with size from 1 to 500 nm, are interesting materials to be used as catalysts, fillers, stabilizers, radiation sensitizers, contrast agents and as drug delivery systems, due to their large surface to volume ratio, which provides large surfaces for interactions with small quantities of material. Their small size allows for efficient penetration into substrates.

The field has exhibited strong growth in past decades. According to SciFinder search made at 20.1.2020, there were three journal articles published in the year 1979, which contained the concept nanoparticle. Similar search for the year 1989 produced 58; for the year 1999, 2800, for the year 2010, 39548 and for the year 2019, 98261 references.

The field is extensive and the nanoparticles themselves exhibit a broad variety of structures with different shapes (spheres, rods, stars and capsules) and being constructed from different materials.[2]

Hard, inorganic nanoparticles, such as superparamagnetic iron oxide particles, quantum dots and plasmonic nanoparticels, including gold nanoparticles, have been studied to aid diagnostics as contrast agents and to act as radiation sensitizers in biomedicine, as well as to introduce added functionality to materials, for example antimicrobial, magnetic and catalytic properties.

Soft nanoparticles such as self-assemblies and crosslinked polymer particles have been of an especial interest for the biomedical field as these materials are able to host guest molecules and able to migrate in the body.[2,3] Soft nanoparticles are also interesting as supports for catalyst due to open penetrable structure that provides access for the reagents to the catalytic site while also providing stability and recyclability to the catalyst.[3-6] Soft nanoparticles may serve as emulsion stabilizers as their deformability allows for efficient coverage of interfaces. Deformable particles can act as impact absorbers at the interfaces to efficiently stabilize emulsion droplets against collision induced coalescence.[5-7] A more extensive description of what type of synthetic soft nanoparticles exist, how they are could be used in the applications is provided in the next chapter.

1.2 SOFT NANOPARTICLES

1.2.1 DIFFERERENT TYPES OF SOFT NANOPARTICLES

Soft nanoparticles are small, deformable and penetrable. In this chapter, few different types of soft particles are introduced including self-assemblies of amphiphiles, mesoglobules and hydrogel particles. All of the aforementioned particle types are discussed in the experimental part of this dissertation.

Self-assemblies of amphiphiles

Amphiphilic compounds have segments with different solubilities, they have solvophobic ("solvent hating") and a solvophilic ("solvent loving") parts.[8,9] In a selective solvent, which is good for a part of the molecule, amphiphiles can form self-assembled structures, to minimize the contacts of the solvophobic part with the solvent. The simplest of such is a spherical core-shell micelle, in which the solvophobic part is buried in the core and surrounded by the extended solvophilic part. Other structures may also be formed, including worms and vesicles depenging on the amphiphile. The structures are presented in Scheme 1.

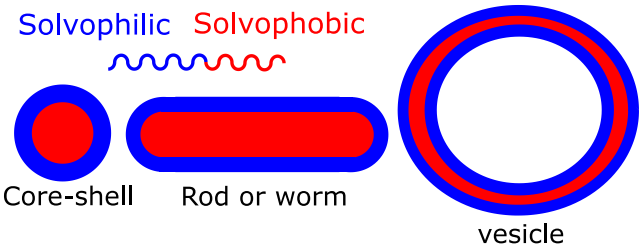

Scheme 1 2D Cross-sections of typical self-assemblies of amphiphiles

A typical feature of the self-assembling is the critical micelle concentration (CMC). CMC is the lowest amphiphile concentration at which micelles are formed. CMC of a common surfactant, sodium dodecyl sulfate (SDS) is 8.1 mM in water at 25 °C. Below this concentration SDS is molecularly dissolved and partly absorbed to intefaces. Above this concentration, SDS forms spherical micelles. The number of micelles increases upon further addition of SDS for a broad concentration range and the micelles are in equilibrium with free SDS molecules in water. The SDS micelle is an example of a self-assembled supramolecular structure formed by small organic compounds. The amphiphile can also be polymer, for example a block copolymer.[8,9]

All self-assemblies are dynamic in nature and alterations in their surroundins may cause changes in their stuctures. To be applicable for cargo

delivery applications, the nanoparticles will need to be stable and robust and to withstand the varying conditions during the delivery path, which may include changes in pH, the presence of proteins, and severe dilution.

The stability of the particles may have thermodynamic or kinetic origin. The self-assembly is thermodynamically stable when it represents the lowest energy state of the system. Self-assembly may also be kinetically stabile, meaning that the assembly is not in its lowest energy state but so slow to reach the thermodynamically stable state that during the application or observation time, the assembly is stable.[8,9]

Size, dispersity and shape of an assembly is affected by the assembly method. Methods for formation of the self-assemblies include gradual solvent change from a good solvent to a selective one (dialysis or cosolvent evaporation), instant exchange of solvent by addition of concentrated amphiphile solution into a selective solvent, and film solvation with a selective solvent.

Mesoglobules

Mesoglobules are a type of amphiphilic self-assemblies. They are colloidally stable, typically 10 to 1000 nm sized, aggregates of responsive polymers formed upon applying external stimuli such as temperature to decrease the solubility of the polymer and hence to induce the self-assembly.[10]

Colloidal gels

Gel is as a "Non-fluid colloidal network or polymer network that is expanded throughout its whole volume by a fluid", as defined by IUPAC.[4] Colloidal gels are discrete gel particles dispersed in a liquid. When the liquid is aqueous, these gels are often referred to as colloidal hydrogels. Independent of the liquid these particles are also often referred to as nanogels (size 1 to 500 nm) or microgels (size 0.1 to 100 μm). Crosslinked amphiphilic assemblies (when expanded throughout by a fluid) can also be considered colloidal gels, but colloidal gels do not necessarily have segments with different solubility. Gels resist molecular dissolution in a good solvent into individual polymer chains due to crosslinking (chemical or physical). Changes in solvent quality affect the swelling degree of the gel particles.[3-6]

Use as carriers

Due to small size, deformability, and ability to host guest molecules, soft nanoparticles may be used as carriers of active substances, such as drugs, continuous phase immiscible reagents and catalysts.

Soft nanoparticle carrier provides the loaded material colloidal stability and recyclability, and can act as a locus of the reaction, *i.e.* as a nanoreactor. Metal nanoparticle catalysts have been loaded into colloidal gels for this purpose.[11] The soft nanoparticles, especially colloidal gels, may also possess surface-active properties and stabilize emulsions.[5] Surface-active soft nanoparticles carrying catalyst, have been used to catalyse reactions at liquid-liquid interphases. This is especially useful in emulsions, as the interphase volume is multiplied compared to that of corresponding macro phases and as a result reaction rates are higher.[12]

In drug delivery, soft nanoparticles are used to solubilize drugs and to increase their bioavailability.[2,3] In addition to this, nanoparticles can be used for delivering a loaded drug to a target site for *in situ* release. This is especially important for cancer drugs, as they are toxic to healthy cells and tissues.[13] More effective delivery of these drugs to the target site means that lower administered dosages can be used, meaning less side effects.

The targeting of cancer drugs to solid tumors is most often "passive" *i.e.* based on the size of the drug vesicles and on a phenomenon called enhanced permeability and retention (EPR) effect. The EPR effect was first described in 1986, when it was observed that relatively large proteins and protein conjugates more effectively accumulated in to a solid tumor tissue in comparison to healthy tissues.[14] The EPR effect is due to the unique vascular characteristics of tumors, which include leaky vessels and poor lymphatic drainage.[14,15] Larger molecules, which are too big to diffuse unspecifically out from blood vessels can escape to tumors do to the leakiness, and accumulate there due to the poor drainage. Small proteins or drugs do not exhibit similar accumulation. Even though this type of passive, size based targeting is beneficial and used in clinical treatments, there is still plenty of room to improve the targeting. According to a recent meta-study on existing literature (prior 10 year period) on nanoparticle targeting, on medium less than 0.7 % of administered dose reached the target.[16]

Another approach to the targeted drug delivery is "active" targeting and it is based on functional groups on the nanoparticles that help to guide the particles to the target sites. Natural nanoparticles such as viruses offer an inspiration for active targeted particles. In general, the surface to volume ratio is large in nanoparticles, and thus large amount of targeting groups is needed to cover the whole surface of particles. Still, if we use viruses as models, we learn that there probably is an optimal surface coverage, which is very different compared to total coverage.[17] Thus, there are many parameters to optimize, especially as changing the surface of nanoparticles probably changes also their colloidal properties.

Softness, meaning deformability, of the drug delivery particles has been also recognized as an important factor, which effects targeting.[18] Anselmo *et al.* studied the effect of elasticity of polyethylene glycol hydrogel particles (elasticity varied between 0.255 and 3 000 kPa) on blood circulation time, biodistribution, antibody-mediated targeting, endocytosis, and phagocytosis. It was demonstrated that the softer counterparts exhibited longer circulation times and more effective targeting. The reason behind the phenomena was attributed to the more effective removal of the stiffer particles by the immune cells (macrophages).[19] Deformability plays also another role as soft nanoparticles can more effectively pass through membranes compared to similar sized hard nanoparticles due to being able to deform to pass through.[20] Thus, soft nanoparticles are more prone to pass biological filters present in the body.

1.3 RESPONSIVE POLYMERS AND SMART SYSTEMS

Smart polymer system is a term used for materials, which conduct a function in respond to changes in their environment[21] As depicted in the previous chapter, soft nanoparticles are often sensitive to their surroundings. Thus, the particles may be used in various smart systems including drug delivery vehicles with on-site drug release, emulsions that can be separated[12] and nanoreactors that can ne turned active or inactive,[22] upon applying stimulus.

From a design point of view, the responsiveness can be incorporated to soft nanoparticles by creating the particles from responsive polymers or from amphiphilic polymers with self-assembly driven by weak interactions or from soluble polymers with reactive chemical crosslinks that break upon applying stimulus. Largest difference between the approaches is the reversibility of the transformation. Colloidal hydrogels of responsive polymers typically recover to their original state after removing the stimulus. Polymer self-assemblies and colloidal hydrogels with reactive crosslink usually do not.

The reversibility of the responsiveness is essential to many applications field including nanoreactors and on-off stabilizers. The reversibility of the responsiveness may also be useful in cargo delivery applications. Generally, the release of a loaded compound from a colloidal gel particle is diffusion controlled.[23] The degree to which the gel network is swollen controls the rate of diffusion into and from the particles. This can be utilized in cargo delivery systems, as the particles can be loaded in the swollen state and a sustained release is observed under conditions where the particles are more tightly packed.

There are several polymers, which exhibit responsiveness in aqueous solutions. Typical stimuli include light, pH, and temperature. Typical response to the stimulus is a change in the solubility of the polymer and correspondingly

soft nanoparticles built of a responsive polymer shrink or swell according to the stimuli.[21]

1.4 POLY(*N*-VINYLCAPROLACTAM)

Poly(*N*-vinylcaprolactam), PNVCL, is a thermoresponsive non-toxic polymer.[24] Structure of the polymer is displayed in Scheme 2. This chapter discusses the most important properties of the polymer, including selected general physical aspects, toxixity and thermoresponsiveness. Synthesis of PNVCL and PNVCL particles are discussed in the following chapters 1.5 and 1.6, respectively.

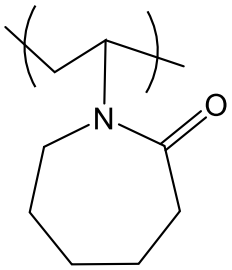

Scheme 2 Structure of PNVCL

1.4.1 GENERAL PROPERTIES

PNVCL is an amphiphilic polymer, with every repeating unit containing a polar amide moiety as a part of a cyclic otherwise aliphatic non-polar ring. As a result of the amphiphilic nature, the polymer is soluble in various non-polar and polar solvents including 1.4-dioxane, tetrahydrofuran, chloroform, various alcohols, benzene, toluene and cold water. The polymer, however, exhibits poor solubility in hexane, diethyl ether and hot water.[24]

In water, the polymer is non-charged, exhibits thermoresponsiveness and is very stable against acidic hydrolysis.[25] It has been reported that only 1.5 mol% of the repeating units of PNVCL were hydrolysed during 60 h at 100 °C in 1 M HCl solution.[25]

Upon drying PNVCL forms films. T_g of dry PNVCL is around 149 °C. Water is a very effective plasticizer for the polymer, 25 weight % (wt%) water content is enough to lower T_g of PNVCL to -17 °C.[26] Carbonyl group of PNVCL acts as an acceptor in hydrogen bonding, which is what the interactions between water and PNVCL are based on.

Similarly, other compounds bearing hydroxyl groups can also form hydrogen bonds with PNVCL. It has been observed that wet PNVCL /oligoethyleneglycol mixtures at right ratios form pressure sensitive adhesive

films.[27] The terminal hydroxyl groups of oligoethyleneglycol bind with PNVCL carbonyl groups, thus resulting in a formation of a network. Hydrogen bonding along with hydrophobic interactions has been used to create PNVCL containing films with layer-by-layer method.[28]

In industry the PNVCL has been used to prevent hydrate formation in natural gas pipelines[29] and it is sold to be used in hair products[30].

1.4.2 CYTOXICITY

PNVCL is is considered non-toxic and safe.[24,31] Author is not aware that any PNVCL containing pharmaceutics would have yet reached the market, despite the vast development work of PNVCL contaning materials for biomedical applications. However, BASF is selling in Europe a PNVCL containing graft copolymer named Soluplus, for solubilizing active pharmaceutical ingredients.[32]

1.4.3 THERMORESPONSIVENESS

Linear PNVCL

PNVCL exhibits thermoresponsive behaviour in aqueous solutions, *i.e.* PNVCL is soluble to cold water (below 29 °C) but becomes insoluble upon heating. The phase transition temperature of PNVCL depends on the concentration and molecular weight of the polymer, increasing either concentration or molecular weight shifts the phase transition temperature to lower temperatures.[33]

Transmittance measurements are used for determining the cloud point. In the measurements an aqueous polymer sample is heated or cooled, and the transmittance of the sample is recorded at a suitable wavelength (usually 600-700 nm). During the heating the solution turns turbid as the polymer becomes insoluble and forms aggregates that scatter light and a decrease in transmittance is observed. The temperature where the transmittance drop starts is reffered to as the cloud point. The transmittance measurements are very useful for comparing polymer samples, and to study the effect of additives on the thermal behaviour of the polymer. Even though a single temperature value, *i.e.* the cloud point, is often used to describe the phase transition, high sensitivity DSC measurements have revealed that the phase transition process is actually gradual and happens within a relatively broad temperature range and that the released heat per NVCL unit is in the range of 4-5 kJ/mol.[34] Sophisticated IR measurements have also shown a gradual phase transition.[35]

NMR, IR and SAXS data combined with quantum chemical calculation have revealed the molecular basis of the transition.[36] Below the phase transition, the polymer is well solvated due to hydrogen bonding between the

amide carbonyl of the polymer and water molecules. Upon heating, the hydrophobic interactions become dominant, and the extent of hydrogen bonding decreases. At the molecular level, PNVCL carbonyl binds two water hydrogens at solvated state and upon heating above the phase transition one of the bound hydrogens is lost. Simultaneously, indirectly bound water (secondary hydration layer) is pushed out from the collapsing polymer coil. Result is that PNVCL collapses with more tightly bound water. According to molecular modelling the conformation of PNVCL changes during phase transition from partly folded to a more folded structure.[37]

The structure and size of the formed aggregates depends on the polymer concentration. Laukkanen et al. have shown that at low polymer concentration (0.1 g/L), the phase separation, *i.e.* aggregation can lead to spherical monodisperse aggregates, mesoglobules.[34] The formed mesoglobules were stable against further coalescence, at least for several days. Sun et al. studied the process with IR methods in D_2O and concluded that stability arises from enrichment of hydrophilic groups on aggregate surfaces, whilst the most hydrophobic domains are buried in the core of the spherical aggregates.[35] At high concentrations, the aggregation leads to the precipitation of the polymer.

Hydrogel PNVCL

In crosslinked water swollen PNVCL networks, *i.e.* hydrogels and colloidal hydrogel particles, the phase transition is referred to as the volume phase transition (VPT). During the VPT the gel shrinks as the polymer becomes less soluble, loses hydration and packs into a more compact conformation. Mikheeva et al. studied the phase transition of a hydrogel grinded to particles and suspended in water.[38] With DSC measurements it was observed that the transition is gradual as with linear PNVCL, but the transition of PNVCL hydrogel consisted of two steps. The lower temperature step was associated with microseggragation of small hydrophobic domains in the PNVCL gels and the higher temperature step was associated with merging of the domains, as the gel particle collapses

Effect of additives

Water solubility of many macromolecules depends on the presence of cosolutes, such as salts (ions).[39,40] More than 100 years ago, Hofmeister reported that ions with same nominal charge can have very different effects on the solubility of proteins, and constructed a series to describe the influence of selected ions. A modified version of the series is drawn in Scheme 3. Ions on the left decrease the solubility, *i.e.* salt-out proteins and the ions on the right, increase the solubility, *i.e.* salt-in proteins. We will discuss effet of ions on the solubility of PNVCL, in respect to this updated Hofmeister series.

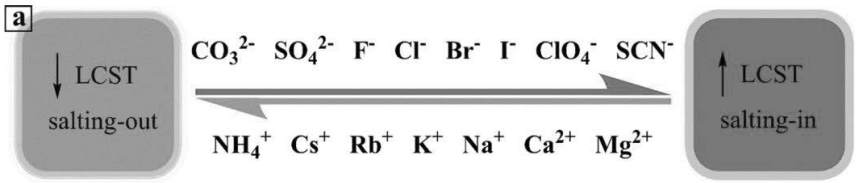

Scheme 3 Updated Hofmeister series and the effect on phase transtition temperature of a thermoresponsive polymer. Reprinted from reference[40], Copyright (2019), with permission from Elsevier.

For PNVCL, effet of anions has been observed to follow the Hofmeister series. Anions at the left hand of the series decrease the phase transition temperature and some of the ions at the right hand side including Br^-, I^- and SCN^- have been shown to increase the transition temperature.[41,42]

Effect of cations on the solubility of PNVCL has been less studied. Generally, the effect of cations to the solubility of non-charged macromolecules is considered to be weaker compared to the effect of the anions. The tested cations have decreased the solubility of PNVCL in the following order, $Al^{3+} > Zn^{2+} > Na^+ > NH_4^+$.[43]

Addition of some non-ionic species, which can bind to PNVCL, has been shown to affect the LCST in aqueous solutions. Addition of methanol, which is a good solvent for PNVCL, to water hardly affects the phase transition until a high concentration (20 mol%) has been reached. Upon this ratio addition of more methanol increases the LCST, finally increasing it to above the boiling point. More bulky aliphatic alcohols (isopropanol, propanol, *tert*-butanol) lower the LCST at low concentrations and increase it at higher concentrations.[25] This cononsolvency behaviour can be explained as follows. At low concentrations, specific interactions between the alcohols and PNVCL reduce those between water and PNVCL, effectively lowering the transition temperature. The effect depends on the bulkiness of the alcohol. At higher concentrations, the added alcohol changes the structure of the bulk solvent and increases the LCST. The interactions between the alcohols and PNVCL are based on hydrogen bonding between the alcohol hydroxyl hydrogen (donor) and the carbonyl group of PNVCL (acceptor) as well as hydrophobic interactions between the alcohols with higher hydrocarbon content and PNVCL main chain and aliphatic ring. Laukkanen et al. have protected PNVCL mesoglobules against dissolution upon cooling by using phenols capable of multiple hydrogen bonds as physical crosslinkers for PNVCL.[44]

Effect of Copolymerization

Copolymerization can be used to tailor the transition temperature of PNVCL.[45] Statistical copolymers of PNVCL with a more hydrophobic comonomer, such as vinyl acetate exhibit lower phase transition temperature compared to the PNVCL homopolymer with similar molecular weight. Vice versa, copolymers with a more hydrophilic comonomer such as *N*-methyl-*N*-vinylacetamide exhibit higher phase transition temperature compared to PNVCL homopolymer. Distribution of repeating units in the copolymer has also a decisive role in determining the degree to which the incorporated comonomer affects the thermal behaviour. Therefore, it is possible to synthesize block copolymers with PNVCL block and another thermoresponsive block, which exhibit two distinct phase transition temperatures, whereas a copolymer with more randomly distributed repeating units along the chain would exhibit only one transition.

1.5 SYNTHESIS OF POLY(*N*-VINYLCAPROLACTAM)

1.5.1 FREE RADICAL POLYMERIZATION

PNVCL is synthesized using radical polymerization of NVCL. The reaction has been performed in various organic solvents and in water, with a variety of initiators and conditions. Depending on the conditions polymers are obtained with molecular weights ranging from oligomers to polymers with Mw up to 1.5 x 10^6 g/mol.[34] A broad molecular weight distribution is however and inherent property of this synthesis method. Precipitation and fractionation can used to obtain a narrower distribution.

Free radical polymerization can be also used to synthesize copolymers of PNVCL. A comprehensive list of comonomers, and copolymerization reactivities is provided in a recent review article about the polymer.[24] In most cases, NVCL is the least reactive of the monomers. This has consequences as in a batch polymerization, the more reactive polymer is polymerized first and this results in long segments of homopolymer and a composition drift during the synthesis.

1.5.2 RAFT

Reversible-deactivation radical polymerizations (sometimes referred to as "controlled" or "living" radical polymerizations)[46] are set of methods, which provide easily tuneable molecular weight of the resultant polymer. With these methods, molecular weight grows linearly with conversion during the polymerization and narrow molecular weight distribution is maintained throughout the synthesis. There are reports of reversible-deactivation radical polymerization of NVCL using cobolt-mediated polymerization[45,47], RAFT polymerization,[48-57] and ATRP synthesis[58,59]. From the aforementioned, the RAFT polymerizations are dicussed in more detail, as it is the only one of the reversible-deactivation radical polymerizations used in the experimental part of this dissertation.

RAFT differs from free radical polymerization by the use of a chain transfer agent (CTA). Chain transfer agent acts as mediator of activity between growing chains. Under the right conditions, this leads to a controlled polymerization, where polymer chains grow at similar pace, and narrow molecular weight distribution is maintained through out the polymerization. In this case, the molecular weight of the polymer can be calculated with equation 1.[60,61]

$$(1) \qquad M_n = \frac{monomer\ concentration\ in\ feed}{CTA\ concentration} * conversion + Mn(CTA)$$

For a successful RAFT polymerization, the choice of CTA is crucial. A common formula for CTA is given in Scheme 4. When Z is oxygen, the CTA is a xanthate and the polymerization can be called macromolecular design via inter-change of xanthate (MADIX) polymerization.

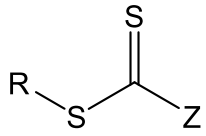

Scheme 4 General structure of a chain transfer agent

Copolymerization with RAFT process can be tricky due to the mechanism of RAFT relying on the reactivity of the active species and monomers rarely have equal reactivities. Synthesis of block copolymers is feasible in the case monomers have equal reactivities to be RAFT polymerized using the same CTA. The order of block formation is also essential to obtain control; the monomer for which polymer has a greater leaving capability should be polymerized first.

1.6 SYNTHESIS OF PNVCL PARTICLES

For the synthesis of PNVCL particles there are two distinct approaches. PNVCL particles can be obtained with the self-assembly of PNVCL or with synthesis methods which directly produce particles. This chapter discusses first the self-assembly method followed by the polymerizations. A comparison between the different methods is provided in the end of this chapter.

1.6.1 SELF-ASSEMBLY

As discussed in section 1.2.3, PNVCL homopolymer may form stable self-assembled aggregates in aqueous solutions upon heating above the thermal transition temperature under dilute conditions. The particle size and size distribution depends on the molecular weight and concentration of the polymer and on the heating program.[10,34,44] The self-assembled structures are stable for days, even months, and the self-assembly process can be used to capture material inside the particles. The particles are dynamic in their nature, stable against dilution, but disassemble by lowering the temperature. However, hydrogen bonding with phenols may be used to make the particles to withstand cooling.[44,62] Similarly, PNVCL-block copolymers can form assemblies upon heating and can be stabilized against heat induced dis-assembly.[63]

In addition to thermoprecipitation, PNVCL block copolymers form assemblies as any amphiphilic block copolymer. In these assemblies PNVCL can be either one, the solvophobic or solvophilic block depending on the other block and on the conditions. PNVCL-PEG copolymer particles have been formed for example both with thermoprecipitation[44] and with solvent-exhange from DMF to H_2O (37 °C).[64] Additionally, PNVCL block copolymers have been self-assembled using nanoprecipitation and by film-dehydration followed by membrane extrusion.[65]

PNVCL has also been assembled with silk fibroin using the layer-by-layer method to form multilayers on silica particles. Hydrophobic interactions and hydrogen bonding are responsible for the interactions between silk fibroin and PNVCL.[28] There exists a recent review about the self-assemblies of PNVCL copolymers for biomedical applications.[66]

1.6.2 PARTICLES BY MEANS OF POLYMERIZATION

1.6.2.1 Precipitation polymerization

Precipitation polymerization is a type of free radical polymerization that is used to make particles, especially colloidal gels. In the polymerization the monomer is soluble in the solvent but the formed polymer is not and as a result, the polymer will precipitate during the polymerization. When synthesising a thermoresponsive polymer, the synthesis temperature is selected such that the formed polymer is insoluble. Surfactants are often used in the synthesis to guide the polymer to precipitate into well-defined, similar sized aggregates, which stay dispersed in the reaction mixture. When synthesizing colloidal gel particles, difunctional comonomers, *i.e.* crosslinkers are used. Then the polymer particles/aggregates formed during the synthesis become permanent polymer networks that do not break even upon improving the solvent quality. Synthesis of colloidal PNVCL hydrogels has been well studied and various comonomers have been incorporated to the particles during the polymerizations. [67-83]

Typically, precipitation polymerizations have been performed as batch polymerizations, meaning that all monomers are present from the start. In batch polymerizations, the reactivity difference between monomers can lead to a composition gradient in the particle structure as the more reactive monomer is incorporated first.[70,71,77,82] For this reason, PNVCL colloidal gels usually have a more crosslinked core and dangling chains on the surface, as the crosslinker, which is the more reactive monomer, has polymerized first.[71,77] Continuous and semi-continuous addition of monomers can be used to control the spatial arrangement of the monomers in the gel particles. Imaz *et al.* and Willems *et al.* have reported syntheses of a homogenously crosslinked hydrogel particles with continued feed of the crosslinking monomer during the polymerization.[71,82]

Precipitation polymerization can also be used to polymerize a PNVCL shell on a pre-existing particle or on a sacrificial template such as a dimethyldiethoxysilane droplet.[84] Removal of the sacrificial template will produce particles with inner lumen, *i.e.* capsules.

1.6.2.2 Emulsion polymerization

Emulsion polymerization is ”Polymerization whereby monomer(s), initiator, dispersion medium, and possibly colloid stabilizer constitute initially an inhomogeneous system resulting in particles of colloidal dimensions containing the formed polymer”, according to the IUPAC definition.[85]

The typical precipitation polymerizations of NVCL in water is also sometimes referred to as an emulsion polymerization. However, in this dissertation the term precipitation polymerization is used for the aqueous polymerizations of NVCL, which are performed above the phase transition temperature of PNVCL, and where the starting NVCL concentration (0.5–3 wt% monomer in respect to H_2O) is close to the solubility limit of NVCL. Most of the PNVCL particle syntheses are precipitation polymerizations. The use of larger concentrations of NVCL has been reported to lead to colloidal instability and to the formation of coagulum during the polymerization.[71]

In addition to precipitation polymerizations in water, PNVCL particles have also been synthesized with miniemulsion[86,87] and inverse miniemulsion polymerizations[88,89]. In miniemulsion and in inverse miniemulsion polymerizations, the initial polymerization mixture consists of evenly sized droplets dispersed in a continuous phase, and these droplets act as the loci of the polymerization and in the end turn in to polymer particles.[90,91] To clarify, the difference between emulsion and miniemulsion polymerization is that in the latter, the starting mixture contains evenly sized droplets that have similar size as the resultant particles. The formation of the initial droplets is achieved by using surfactants and by intensive mixing processes such as sonication. The dispersed droplets often need to be stabilized against Ostawald ripening by using a costabilizer, which is a compound that is highly insoluble to the continuous phase, but soluble to the monomer phase.

In inverse miniemulsion polymerizations, the dispersed droplets consist of a polar solvent (usually water) and the monomer, and the continuous phase is non-polar. This method is suitable for the synthesis of watersoluble polymers. When the polymerization takes place in the droplet phase instead of the continuous water phase, polymer particles are formed instead of a macrogel. Effective incorporation of water-soluble compounds to the formed PNVCL colloidal gel particles could be a reason to use this syntheses method.

In miniemulsion polymerization, the dispersed phase is organic and contains the monomer, and the continuous phase is aqueous. The method has been used for the synthesis of PNVCL particles with high monomer concentrations (up to 16 wt% in respect to H_2O)[86,87] and to synthesize PNVCL particles with a water insoluble comonomer,[92] which can be difficult with precipitation polymerization. The miniemulsion polymerization often demands the use of an additional hydrophobe (costabilizer) such as hexadecane and possibly the use of a cosolvent for the formation of the dispersed phase. The additives can result in a need of extensive purification steps. There is however, two reports of miniemulsion like polymerization of

NVCL without any cosolvent or costabilizers,[92,93] with CTAB as the stabilizer and with starting NVLC concentration <1.4 wt% performed after homonogenization with a microfluidisizer (at least 1100 bars and 8 cycles). The polymerization conditions are close to equal to the ones used in the precipitation polymerizations, except for the homogenization process. NVCL is soluble in water at the used concentration, however relatively stabile (at least for 250 min) monomer/surfactant droplets were observed with dynamic light scattering before addition of the initiator. This was because of the slowness of the dissolution of NVCL in water. This raises a question about the homogeneity of the starting situation in the precipitation polymerizations and on the correctness of the use of the term. In studies on the precipitation polymerization of NVCL, the starting mixture has seldom been investigated to verify the homogeneity.

1.6.2.3 Polymerization induced self-assembly

Polymerization induced self-assembly (PISA) is a type of controlled polymerization, where a solvophilic polymer is chain extended with a solvophobic block.[94,95] During the polymerization the growth of the solvophobic block causes the polymer to self-assemble. The polymerizations are most often RAFT polymerizations, where a solvophilic macromolecule with a CTA end group, *i.e.* macromolecular CTA (macroCTA), is used to control the polymerization and as the soluble block in the forming copolymer. This is also a synthetic route to obtain polymer particles. These particles are not polymer networks but amphiphilic self-assemblies consisting of block copolymers with narrow molecular weight distributions. Usually, no surfactant is needed in addition to the soluble polymer to be chain extended. Other appealing aspect of the polymerization is the possibility to obtain different well-defined morphologies by changing the block length ratio and concentration of the polymerization. Typically, also high monomer concentrations (10 to 30 wt%) can be and are used in the PISA polymerizations.

This dissertation describes the first example of PISA of NVCL as the sole monomer (paper III). Prior work has shown how a partial utilization of the PISA concept can also be beneficial compared to the precipitation/emulsion free radical polymerizations. Etchenausia et al. have synthesized cationic hydrogel particles by polymerizing NVCL in water above the phase transition themperature of PVCL with crosslinker and a cationic macroCTA.[96] Using a crosslinker in a batch polymerization makes it unlikely to obtain a controlled polymerization and hence the polymerization induced self-assembly. However, the synthetic approach proved to be suitable for the production of colloidal hydrogel particles at high monomer concentrations (up to 10 wt% in respect to mass of H_2O) compared to a free radical precipitation polymerization counterpart (no CTA, just surfactants). The macroCTA group reacted during the polymerization and imparted unprecented stability to the

system against coagulation. Same group also performed aqueous PISA copolymerization of NVCL and vinylacetate with a PEG based macroCTA.[97] Control over molecular mass was limited and only few polymerizations were made, but the resultant material was still interesting as the formed polymers resembled by composition Soluplus[32] (see chapter 1.2.2). No crosslinker was used as the hydrophobic comonomer prevented the dissolution of the formed assembly upon cooling if used in sufficiently high amounts (47 mol% of monomers in feed).

1.6.3 COMPARISON OF THE SYNTHESIS METHODS

Various aspects of the different synthesis methods to obtain soft PNVCL nanoparticles are presented in Table 1, to allow convenient comparison between them.

Table 1 *Various selected aspects of synthesis methods of PNVCL particles*

Method	Concentration[a]	Suitable for	*Surfactant*[b]	REF.
Self-assembly	≤ 0.2 wt%	homo- and copolymers	*not used*	10,28,34,44,63,65
Precipitation polymerization	0.5–3 wt%	homo and copolymers	*0–8 wt%, or surfactant type comonomer (2 – 50 wt%)*	67-73,75-83,I, II
Miniemulsion polymerization	≤ 16 wt%	homo- and copolymers	*0.4-2 wt% + possibly an additional costabilizer*[c]	86,87,92,93
Inverse miniemulsion polymerization	≤ 5 wt%	homo- and copolymers	*100 wt%*	89
PISA	1–30 wt%	copolymers	macroCTA	96,97, III

a) monomers in respect to the weight of solvents plus continuous phase,
b) wt% given in respect to monomer weight

2 OBJECTIVES

Work described in this dissertation aims for the development of soft PNVCL particles to be used as carriers of active compounds such as catalysts and drugs. Focus is on the colloidal properties and functions on the outer parts of the particles as these govern the applicability of the particles. The main objective was divided into the following.

1. Preparation of surface functionalizable PNVCL nanogel particles
2. Functionalization of the nanogels with gold nanoparticles to obtain multiresponsive and easily detectable hybrid colloidal gel particles
3. Functionalization of the nanogels with biorelevant moieties, *i.e.* carbohydrates
4. Investigation of the ability of the different nanogels to carry and release guest molecules
5. Investigation on how functionalization affects the morphology and colloidal properties of the nanogels
6. Investigation of PISA of NVCL as an alternative syntheses method to obtain soft PNVCL particles

3 EXPERIMENTAL

In this section the most important experimental procedures and characterization methods are briefly summerized. Detailed descriptions are available in the respective publications, paper I, II and III and their supporting information documents.

3.1 SYNTHESIS

3.1.1 SYNTHESIS OF PNVCL NANOGELS

Nanogels, PNVCL and PNVCL-PA, were synthesized using precipitation polymerization, see Scheme 5. The reaction was performed in 500 ml reactor with 500 rpm motor stirring. Reagent amounts are presented in Table 2.

Water was used as the continuous phase (200 ml per reaction). $NaHCO_3$ was used to keep the pH of the reaction mixture above 7. Polymerization temperature was 70 °C. A bifunctional comonomer, *N,N'*-bis(acryloyl)cystamine (BAC), was used in the synthesis in order to obtain crosslinked particles. Sodium dodecyl sulfate (SDS) was used for stabilization of the formed particles during polymerization and to adjust the particle size. Methacrylic acid (MAA) was used as a comonomer to further stabilize the formed particles. Potassium persulfate (KPS) was used as initiator.

In the syntheses of PNVCL and PNVCL-PA nanogels NVCL, NaHCO3, MAA, SDS, and most of the H_2O where mixed together, bubled with nitrogen and heated to 70 °C after which KPS was added to start the reaction. In the synthesis of PNVCL-PA, 1 h after the reaction had started, propargyl acrylate (PA) was added to the reaction mixture to obtain nanogels with alkyne functions on their surfaces. Overall, the reaction time was 23 h in both polymerizations. The reaction mixture was purified with dialysis. The dispersion was freeze dried to obtain dry product.

Table 2 *Amount of reagents used in the feed of precipitation polymerizations*

Product	**C(NVCL)** (g/L)	**$NaHCO_3$** (wt%[a])	**MAA** (wt%[a])	**SDS** (wt%[a])	**BAC** (wt%[a])	**KPS** (wt%[a])	**PA** (wt%[a])
PNVCL	10	2.5	1	2.5	1	2.5	0
PNVCL-PA	10	2.5	1	2.5	1	2.5	5

a) In respect to NVCL in the feed

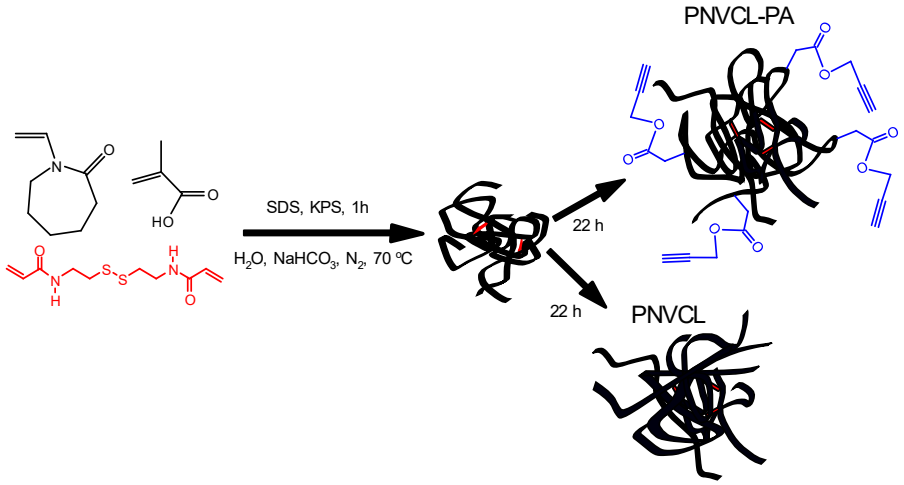

Scheme 5 Syntheses of PNVCL and PNVCL-PA nanogels

3.1.2 FUNCTIONALIZATION OF NANOGELS WITH GOLD NANOPARTICLES

Gold nanoparticles (AuNPs) bearing mercaptoundecanoic acid and azidoundecanothiol ligands was attached to PNVCL-PA nanogel using copper catalyzed azide-alkyne cycloaddition (CuAAc) to obtain the hybrid particle PNVCL-AuNP. 20 mg of PNVCL-PA in 0.1M phosphate buffer was mixed with 5 mg of AuNPs in 2 ml of ethanol. After replacement of oxygen with nitrogen bubling, catalyst precursor ($Cu(OAc)_2$ x $6H_2O$) was added with a reducing agent (sodium ascorbate) to produce the active catalyst (Cu(I)) *in situ*. Reaction was continued 46 h. Schematic presentation of the functionalization is presented in Scheme 6.

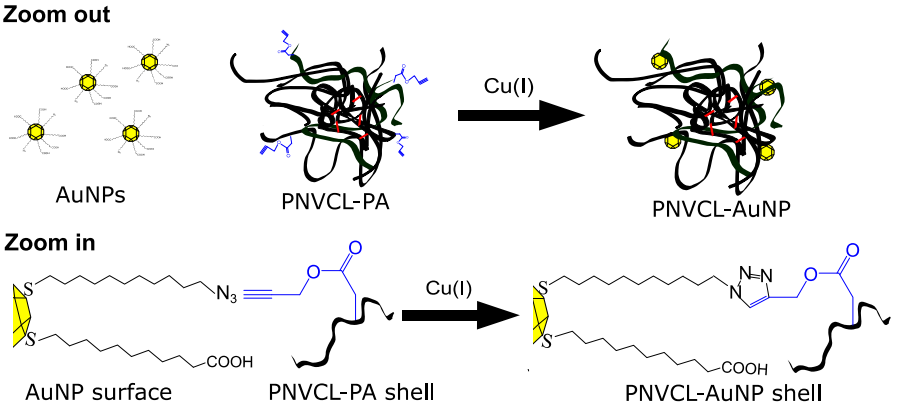

Scheme 6 Functionalization of PNVCL-PA nanogels with AuNPs using CuAAc

A copper chelator EDTA was added, after which the reaction mixture was dialysed against water for 3 days. After dialysis, unstable particles were removed with centrifugation at 15 °C. To separate unmodified AuNPs and PNVCL-PA particles from the product PNVCL-AuNP, a series of liquid / liquid extractions were performed. The 60 ml dispersion was extracted with 70 ml of dichloromethane (DCM) to remove unreacted PNVCL-PA. Then NaCl was added to the aqueous dispersion to obtain 0.1 M NaCl concentration and another extraction was made with 70 ml of dichloromethane. Now the product moved to the DCM phase. DCM phase was washed with H_2O, 0.1 M phosphate buffer and 0.1 M acetic acid. Organic phase was concentrated and diluted with ethanol. Procedure was repeated trice to replace DCM with ethanol. Ethanol exchanged with H2O with dialysis. The dispersion was concentrated in a rotary evaporator to yield 12.5 ml of 1 mg/ml PNVCL-AuNPs dispersion. Part of the dispersion was freeze dried to obtain a dry sample for a thermogravimetric analysis.

3.1.3 FUNCTIONALIZATION OF NANOGELS WITH CARBOHYDRATES

PNVCL-PA was functionalized with the carbohydrate azides displayed in Scheme 3. The carbohydrate functionalized PNVCL-PA gel particles are named PNVCL-Glc, PNVCL-Glc-TEG, PNVCL-Mal and PNVCL-Mal-TEG, depending on the carbohydrate azide.

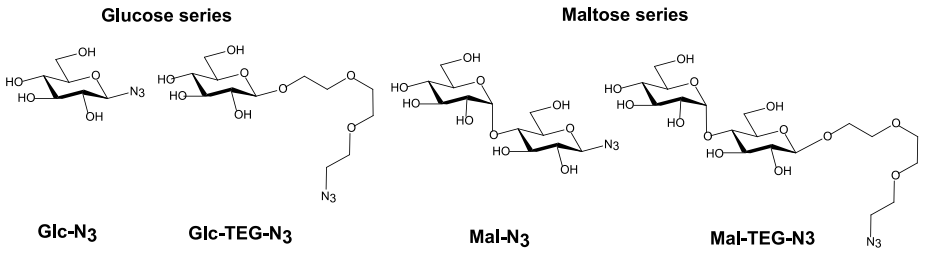

Scheme 7 Carbohydrate azides used for functionalization of PNVCL-PA using CuAAc

The conjugation reaction, CuAAc, was performed in phosphate buffer.
PNVCL-PA (50 mg) and buffer where mixed with the corresponding carbohydrate azide prior to addition of catalyst. Carbohydrate azides were used in excess in respect to PA content estimation of PNVCL-PA. Catalyst was produced *in situ* by reducing copper (II) to copper (I) with ascorbate. Carbohydrate ligand was used for solubilizing Cu (I). The reaction time was 48 h. Particles were purified with dialysis (MWCO 12–14 00 g/mol) against water.

After dialysis and freeze drying the product was obtained in 45 to 55 mg yield depending on the carbohydrate azide.

3.1.4 SYNTHESIS OF PNVCL PARTICLES USING PISA

PISA polymerizations were performed at 50 °C in aqueous 0.1 M TRIS buffer, pH=7.4, see scheme 8 in the result section. PEG based macroCTA was used to control the polymerization and as a sole surfactant in the polymerization. 2,2`-azobis[2-(2-imidazolin-2-yl)propane]dihydrochloride (VA-044) was used as the initiator. Reaction variables studied were the following, overall concentration (reagent ratio constant), initiator concentration (concentration of other reagents constant) and macroCTA to NVCL ratio (NVCL concentration and initiator to macroCTA ratio constant).

Small aliquots where withdrawn from the reaction mixture for conversion analysis and after the reaction was completed a fraction was stored at 50 °C for particle size and shape analysis and the rest of the polymerization mixture was cooled and purified with dialysis (MWCO 3500 Da). Part of the reaction mixture stored at 50 °C was diluted with concentrated salicylic acid at 50 °C to get assemblies which are stable also at room temperature due to hydrogen bonds formed between salicylic acid and PNVCL.

3.2 CHARACTERIZATION

3.2.1 IR, NMR AND UV-VIS

Infrared spectra (IR) were recorded using a Perkin Elmer Spectrum One FT-IR spectrometer with ATR accessory.

The nuclear magnetic resonance (NMR) spectra were recorded with a Bruker Avance III NMR spectrometer (1H: 500.13 MHz, 13C: 125.76 MHz). The probe temperature during the experiments was kept at 23 ˚C. Chemical shifts were calibrated relative to the residual solvent signals.

UV-vis spectra were recorded with a Shimadzu UV-1601PC spectrophotometer or with a Jasco V-750 spectrophotometer.

TGA measurements were performed with Mettler Toledo TGA 850 under nitrogen atmosphere (flow rate 50 ml/min) at heating rate 10 °C/min in the temperature range from 25 °C to 800 °C. Sample mass was 3.5-4 mg and measurements were performed using 70 µl Al_2O_3 crucibles.

3.2.2 LIGHT SCATTERING

Mean hydrodynamic diameter (D_h) and polydispersity (PD) of PNVCL, PNVCL-PA and PNVCL-PA based functionalized nanogels were determined using a Malvern Zetasizer Nano ZS (laser wavelength: 633 nm, scattering angle: 173°). Measurements were performed from 16 to 79 °C at 3°C intervals equilibrating 15 min at every measured point. Samples were equilibrated in a fridge overnight and filtered with a 1 μm glass fiber syringe filter before the measurements.

Hydrodynamic diameter distributions were obtained with CONTIN from measurements at 90° angle using a setup consisting of a Brookhaven instrument BI-200SM goniometer, BICTuboCOrr digital pseudo-cross-correlator and a BI-CrossCorr detector including two BIC-DS1 detectors. The pseudo-cross-correlation functions were collected in a self-beating method. For analysis of PISA products and PNVCL-sugars, the used light source was Coherent Sapphire 488 nm blue laser with incident light set between 10 to 30 mW. For analysis of PNVCL-AuNPs the light source was BI-mini L140 at 637 nm, operated with 50% power, incident light 70 mW. The sample cell temperature was controlled with a Lauda RC 6 CP thermostat. To study the shape of particles measurements were repeated at multiple angles.

3.2.3 FLUORESCENCE

Horiba Jobin Yvon Fluoromax-4 spectrofluorometer was used for the fluorescence measurements. Quartz cuvettes with 10 mm path length were used. Two different fluoresecence probes were used: 8-anilino-1-naphtalenesulfonic acid (ANS) and 4-(dicyanomethylene)-2-methyl-6-(4-dimethylaminostyryl)-4H-pyran (4HP). Emission spectra were measured at different temperatures ranging from 16 to 73 °C in 3 degree intervals, after 15 min of stabilization at each temperature.

ANS samples were prepared from 2 ml 0.25 mg/ml polymer in 10 mM HEPES solutions by adding 2 μL of 10 mM ANS aqueous solution and mixing overnight. Emission was measured with 379 nm excitation using 1 nm excitation and 2 nm emission slits. Blank measurements were performed with samples before additions of the fluorescent probe and this data was subtracted from the sample spectra.

4HP samples were prepared by adding 6.6 μl of 10 mM 4HP chloroform solutions to empty vials, which were then dried under nitrogen flow. 2 ml of 0.25 mg/ml polymer in HEPES solution was added to the vials and the solutions were kept in refrigerator for at least 2 days prior to measurements. For 4HP, fluorescence emission was measured with 470 nm excitation using 1 nm excitation and 2 nm emission slit widths.

3.2.4 CRYOGENIC TRANSMISSION ELECTRON MICROSCOPY

PNVCL-AuNPs were analyzed using JEM 3200FSC cryo-transmission electron microscope (Jeol) operated at 300 kV in bright field mode. Images were acquired with a CCD camera (Gatan) using an Omega-type Zero-loss energy filter, while the specimen temperature was kept at -187 °C. Samples were prepared using FEI Vitrobot Mark IV from 3 µl aliquots on 400 mesh lacey or holey carbon copper grids under 100% humidity, then blotted two times with filter paper for 1.5–2.5 s and subsequently plunged into -170 °C ethane/propane mixture. ImageJ software was used to analyse size of particles from the images. The average size was calculated based on over 1000 AuNPs measured.

SA stabilized PISA products were observed with a FEI Talos Arctica microscope operated at 200 kV. The images were recorded at a magnification of 57 000× with a FEI Falcon 3 camera operating in linear mode. Samples were prepared with a Leica EMGP vitrification device from 3 µl aliquots on freshly glow-discharged Quantifoil R2/2 grids.

3.2.5 SEC

Size exclusion chromatography (SEC) measurements were performed with Waters ACQUITY APC apparatus connected to an ACQUITY refractive index detector. The flow rate was 0.6 ml min^{-1}. The columns used were ACQUITY APC columns of 200 Å, 450 Å and 900 Å. Measurements were performed at 30 °C. The eluent was THF. Low dispersity PMMA samples were used as a reference.

3.2.6 INTERACTION STUDIES WITH A CARBOHYDRATE BINDING PROTEIN

The accessibility of the carbohydrates on the gel particles for biorelevant interactions was studied with a precipitation assay. Aliquots of concentrated particle dispersion (6 µl of 50 mg/ml nanogel dispersion) was added per 1 ml of concanavalin a (Con A) solution. As a result of the protein, Con A, binding several sugar moieties the particles aggregate with the protein. After 30 min, the particles and aggregates were removed from dispersion centrifugation 20 min 10 000 rpm, 9391 rcf. The supernatant was weighted, and its lectin concentration was determined from UV absorbance before the next nanogel addition.

3.2.7 SALT INDUCED AGGREGATION

Salt induced aggregation was tested at 50 °C with 1 mg/ml aqueous nanogel samples. Aqueous NaCl (2 µl of 2 M) was added per 1 ml of nanogel dispersion. After a 15 min stabilization, the transmittance was measured and then, the next aliquot of saline water was added. Transmittance at 650 nm was plotted against salt concentration to find the aggregation and precipitation concentrations. The aggregation point was the NaCl concentration where the transmittance discontinuously decreased. The precipitation point was determined as the concentration where the visible precipitation appeared or where the transmittance had increased compared to the previous addition.

3.3 RESULTS AND DISCUSSION

3.3.1 PRECIPITATION POLYMERIZATION OF NVCL

PNVCL and PNVCL-PA nanogels were obtained in 50-60 % gravimetric yields in respect to total monomer mass in the feed. Charateristic absorbance bands of PNVCL were seen in the IR spectra of both particles. The incorporation of PA to PNVCL-PA was also confirmed by the IR studies, as there is a band originating from the carbonyl of PA at 1736 cm^{-1}, see Figure 1.

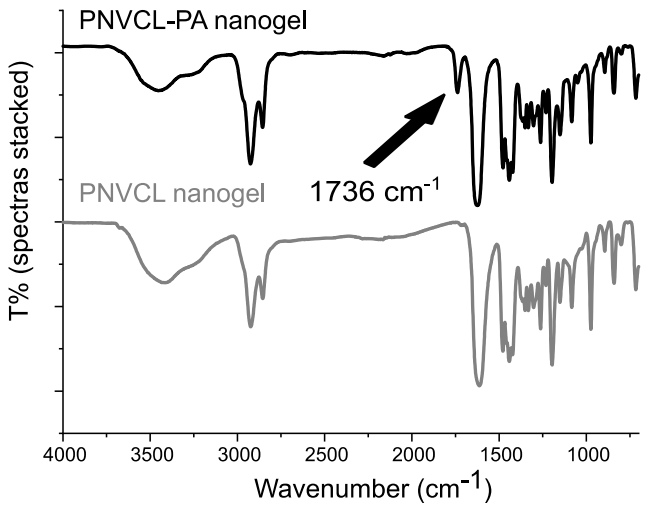

Figure 1 IR spectra of PNVCL-PA and PNVCL nanogels[II]

To ensure the propargyl functions are incorpoprated to the shell of the gels, the synthesis of PNVCL-PA was performed in two steps. According to conversion sampling and analysis with ^{1}H NMR, the NVCL conversion was 57% at the time of PA addition and the final NVCL conversion was 67%. This means that approximately 85% of the final NVCL conversion had been reached at the time of PA addition to the reaction mixture.

Thermoresponsiveness of the PNVCL and PNVCL-PA particles were studied with light scattering. Hydrodynamic diameter of the particles plotted against temperature is presented in Figure 9. The PNVCL-PA particles shrank upon heating, which is typical for PNVCL based gel particles. The PNVCL particles however, formed aggregates upon heating. This is typical for linear PNVCL and slightly crosslinked PNVCL. PA seems to add crosslinking points to the gel particles by hydrophobic interactions or by reaction of the alkyne function of PA.

3.3.2 NANOGELS DECORATED WITH GOLD NANOPARTICLES

Gold nanoparticles protected with mercaptoundecanoic acid and azidoundecanothiol were bound to the gel particle surfaces (Scheme 6). The azide bearing ligands reacted with the propargyl alkyne groups on the PNVCL-PA particles. The mercaptoundecanoic acid ligands gave the gold particles water dispersibility above pH=6.1 (paper I, Fig. 6).

To obtain information about the amount of AuNPS on the PNVCL-AuNP particles, thermogravimetric analysis (TGA) was performed. Organic material in PNVCL-PA, AuNPs, and PVNCL-AuNPs was pyrolyzed by heating to 800 °C and the mass losses were compared (Figure 2). According to calculation (paper I, supporting materials), the AuNPs content of the PNVCL-AuNPs was 30 wt%, which is close to the ratio used in the feed (20 wt%) considering the 50 wt% gravimetric yield after purification. Most of AuNPs (75 wt%) in the feed were included in the product, whilst only 44 wt% of the PNVCL-PA in the feed ended into the purified product.

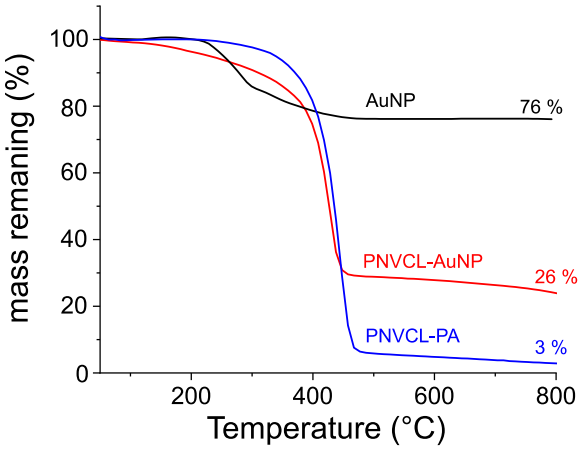

Figure 2 Thermogravimetric analysis results for AuNPs, PNVCL-AUNPs and PNVCL-PA[I]

AuNPs in the PNVCL-AuNPs were seen in the cryogenic transmission electron microscope images, see Figure 3. More images can be found in paper I and in its supporting information. AuNPs give strong contrast in electron microscopy and in the figures of PNVCL-AuNPs, AuNPs are seen as dark dots. According to image analysis the average size of the AuNPs was 2.8 nm. The nanogel part of PNVCL-AuNPs gives less contrast and is seen as light gray spherical object in the images. The size of the light gray part of the PNVCL-AuNPs, was on an average 130 nm. This is seen to represent the denser core of the gels as the size is significantly smaller than the hydrodynamic diameter obtained with dynamic light scattering (Figure 4). The dangling chains did not give enough contrast to be seen in the cryo-TEM images, but AuNPs connected to them were seen.

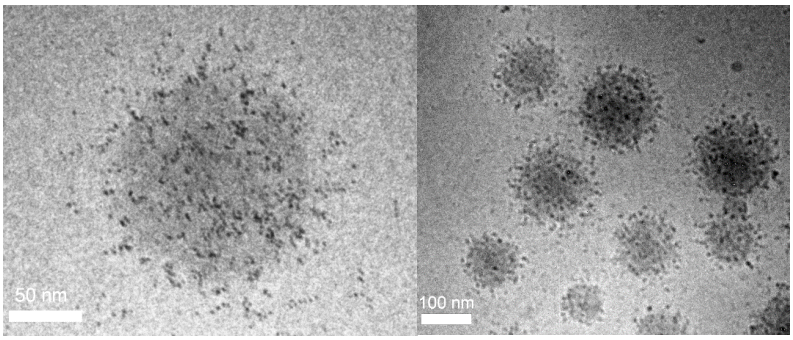

Figure 3 Cryogenic electron microscopy images of PNVCL-AuNP with two different magnefications

3.3.2.1 *Stimuli responsiveness of PNVCL-PA and PNVCL-AuNPs*

Light scattering studies were used used to analyze the thermal response of the PNVCL-PA and PNVCL-AuNP nanogels. The particles shrank upon heating in 10 mM HEPES as did the PNVCL-PA as well (Figure 4). However, the PNVCL-AuNPs were larger at all temperatures and had a broader, bimodal size distribution (see Figure 5). This indicates a partial loosening of the network structure and existence of different sized gel particles. The loosening is because of the reduction of the disulfide links in the the crosslinker (BAC). Reductive conditions were used in the conjugation of AuNPs to the PNVCL-PA particles. A model reaction to verify the hypothesis was conducted and is presented in the supporting information of paper I.

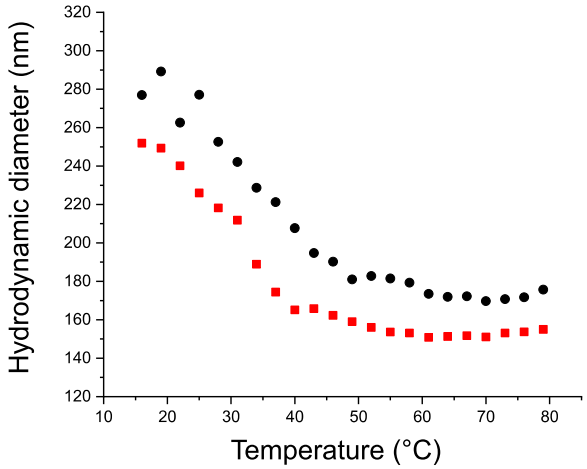

Figure 4 Hydrodynamic diameter (intensity mean average) of PNVCL-PA (■) and PNVCL-AuNPs (●) (0.25 mg/ml) in 10 mM HEPES (pH=7.4) as a function of temperature[I]

The AuNPs introduced new responsiveness to the colloidal hydrogel particles. The PNVCL-AuNPs shrank in addition to heat also in response to oscillating blue light, see Figure 5. The reason for the blue light responsiveness of the PNVCL-AuNPs is the surface plasmon absorbance of the AuNPs. Energy absorbed as light was released as heat from the AuNPs and the heat caused PNVCL to shrink. The PNVCL-PA particles without gold did not react to the blue light exposure.

Oscillating electric field also made PNVCL-AuNPs to shrink (Figure 5). In literature, there is a lot of discussions about the extent and the mechanism by which AuNPs heat in oscillating electric and magnetic fields.[98-100] For small gold nanoparticles, such as those present in PNVCL-AuNPs, electrophoretic heating which is caused by the movement of charged objects in the electric field, seems to be the most plausible explanation. As seen in Figure 5, the PNVCL-PA particles also shrank in the oscillating electric field. PNVCL-PA particles contain charged groups originating from the MAA comonomer and from the initiator (KPS) and thus may heat with the same mechanism. PNVCL-AuNPs have additional charges originating from the mercaptoundecanoic acid ligand on the AuNPs. The additional charges explain why the PNVCL-AuNP shrink more than the PNVCL-PA particles.

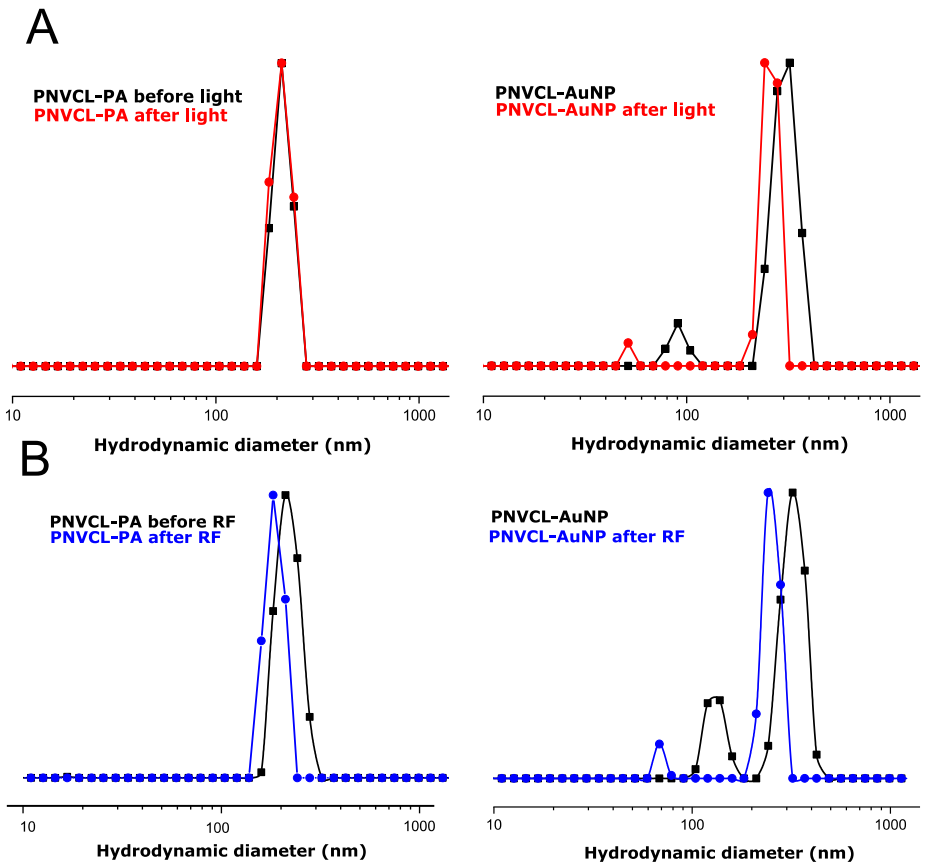

Figure 5 Size distribution of PNVCL-PA and PNVCL-AuNPs before and after exposure to blue light (row A) or oscilating electric field (row B)[I]

The binding and release of two fluorescent probes into and from the gel particles was studied as function of temperature. The first of the probes, 8-anilino-1-naphtelenesulfonate (ANS) is water soluble and exhibits strong fluorescence when bound to a polymer or to a membrane and is practically non-fluorescent in water.[101,102] The second probe, 4-(dicyanomethylene)-2-methyl-6-(4-dimethylaminostyryl)-4H-pyran (4HP) is insoluble in water but binds to the polymers and particles. Both probes are sensitive to the polarities of their environments and in addition, 4HP is known for its sensitivity to the microviscosity.[103-105]

The fluorescence measurements show that both probes bind to the gel particles at ambient temperature but behave differently upon heating. ANS gets expelled into the water phase whereas 4HP keeps bound to the particles. It is worth noting, that the AuNPs quench the fluorescence of the probes (Figures 6 and 7). The experiments are discussed in detail in paper I.

The results highlight the importance of the miscibility of the loaded compound with the continuous phase on its release behavior.

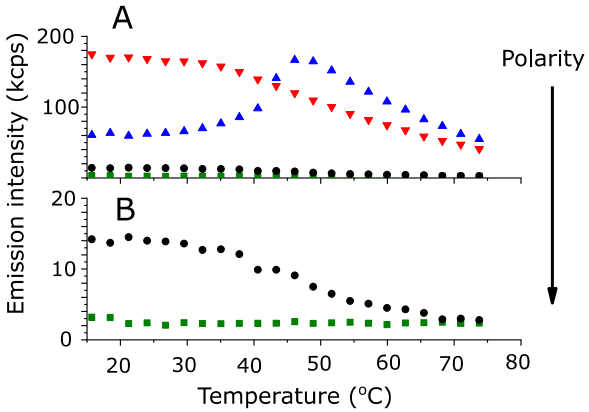

Figure 6 Fluorescence emission of ANS in 10 mM HEPES buffer (A) with no polymer (■),Linear PNVCL (▲), PNVCL-PA (▼) and PNVCL-AuNPs (●). B shows higher magnification for no polymer (■) and PNVCL-AuNPs (●).[I]

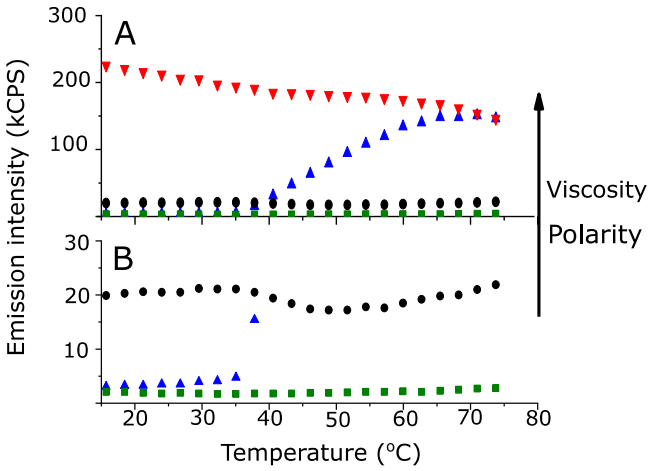

Figure 7 Fluorescence emission of 4HP in 10 mM HEPES buffer (A) with no polymer (■), Linear PNVCL (▲), PNVCL-PA (▼) and PNVCL-AuNPs (●). B shows higher magnification for no polymer (■) and PNVCL-AuNPs (●).[I]

The results show that the nanogels have potential as carriers of hydrophilic compounds with temperature dependent release and also as carriers of hydrophobic compounds in aqueous solutions. These are, however, preliminary tests and more comprehensive loading and release tests would be needed to learn on the extent to which the particles can be loaded and to study the cargo release in a more quantitive manner.

3.3.3 FUNCTIONALIZATION OF PARTICLES WITH CARBOHYDRATE AZIDES (PAPER II)

PNVCL-PA nanogels were also functionalized with carbohydrates. The success of the functionalization was oberved with ^{1}H NMR. Spectrum of PNVCL-Glc is shown in Figure 8. Spectra of other carbohydrate functionalized nanogels can be found in the supporting information for article II (Figures S13-S15). The formation of the triazole moieties were seen from peaks at 8.3 ppm and 5.2 ppm in all of the ^{1}H NMR spectra (H_a and H_b in Figure 8). Integrals of the peaks were used to calculate the molar ratio of carbohydrates in respect to NVCL in the products. According to the analysis there are 4 mol % of attached carbohydrate molecules in respect to NVCL units in all the carbohydrate conjugates. This is believed to represent all of the alkyne moieties in the PNVCL-PA nanogels as in the conjugation reaction, excess of carbohydrate azides and long reaction times were employed. There was 6.7 mol% of PA (in respect to NVCL) used in the feed for synthesis of PNVCL-PA. Thus, some of the PA was not attached to the nanogels during the polymerization or some of

the alkyne functions of PA reacted with radicals and formed extra crosslinks to the polymer particles.

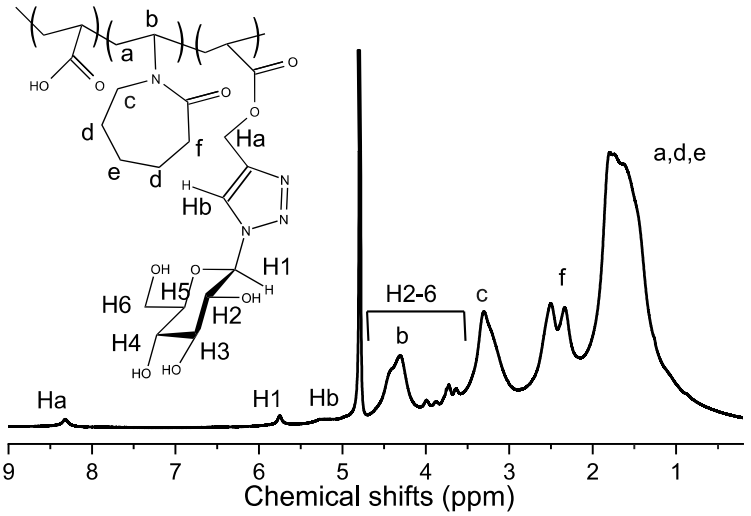

Figure 8 ^{1}H NMR spectrum of PNVCL-Glc in D_2O

3.3.3.1 Size and shape of carbohydrate functionalized particles

Size of the carbohydrate functionalized PNVCL-PA nanogels as well as PNVCVL and PNVCL-PA nanogels were studied with dynamic light scattering as a function of temperature, see Figure 9. The figure displays also hydrodynamic diameter distributions of the samples measured at 25 °C. PNVCL nanogel and PNVCL-PA nanogels were similarly sized at 25 °C, but had very different thermoresponsive behavior. PNVCL nanogels formed aggregates upon heating. This behavior is typical for linear PNVCL and for nanogels with low crosslinking degree and was already discussed. PNVCL-PA exhibited thermoresponsive behavior typical to crosslinked PNVCL nanogels, the volume phase transition. The PNVCL-PA derived carbohydrate decorated nanogels also shrank upon heating, but were larger than the PNVCL-PA at all temperatures. The size distributions were also broader. Carbohydrates made the particles swell by making them more hydrophilic. Some crosslinks (disulfide of BAC) may also have been reduced during the conjugation reaction.

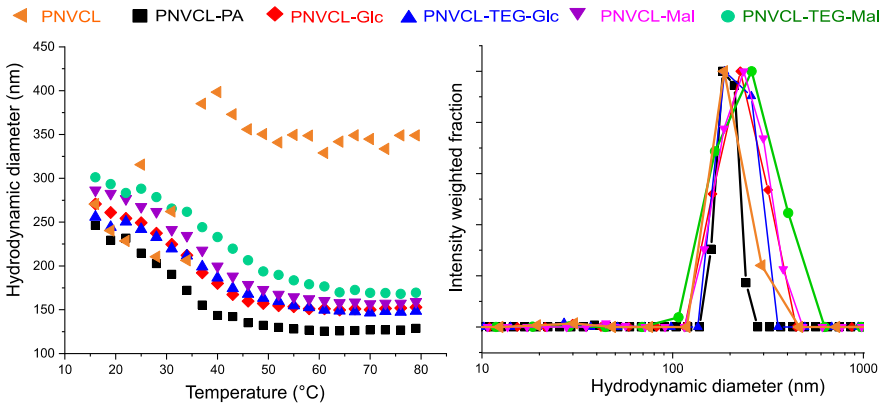

Figure 9 Hydrodynamic diameter of PNVCL, PNVCL-PA and carbohydrate functionalized nanogels; PNVCL-Glc, PNVCL-TEG-Glc, PNVCVL-Mal and PNVCL-TEG-Mal as a function of temperature on the left, Hydrodynamic diameter distributions measured at 25 °C at 90° angle on the right.

The shapes of the carbohydrate decorated nanogels, as well as the original PNVCL-PA particles and neat PNVCL nanogels were studied at room temperature with multi-angle light scattering. The angular dependencies are depicted in Figure 10 with suitable models. The results clearly demonstrate the differences in the morphologies of the particles. The PNVCL nanogel has the most open / extended structure. The carbohydrate functionalized nanogel, PNVCL-TEG-Mal, is more closed. The PNVCL-PA is the most compact. The difference between the particles indicates that there are more crosslinking points in both PNVCL-PA and in PNVCL-TEG-Mal compared to PNVCL nanogel. This supports the hypothesis that some of the alkyne groups of PA may have reacted during the polymerization and formed crosslinks.

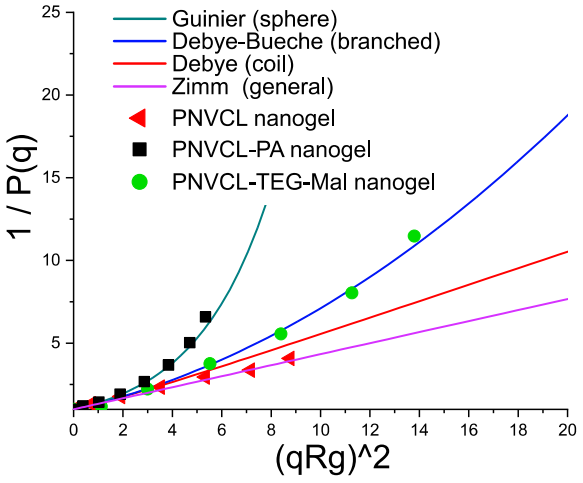

Figure 10 Inversed particle scattering function [P(q) is a function of normalized scattering intensity, $P(q) \equiv I(q)/I\ (q = 0)$] plotted against a squared scattering vector ($q = (4\pi n_0/\lambda)\sin\theta/2$) times squared radius of gyration (Rg). Solid lines represent theoretical curves for selected geometries of scatterers.[II]

3.3.3.2 Stability of PNVCL nanogels against salt induced aggregation

Attachment of carbohydrates to the gels turned the particles more hydrophilic and made the gels to swell. Considering the colloidal stability of the particles, one first wants to know how stable they are against salt addition. Thus, the stability of the nanogels against NaCl induced aggregation was tested at 50 °C and results are presented in Figure 11. In the figure, transmittance of 1 mg/ml nanogel solution is plotted against NaCl concentration. Upon addition of salt, the transmittance decreases as the polymer becomes less soluble and scatters more. The end point of the additions represents the precipitation concentration as at that point the transmittance is higher compared to a previous measuring point. At this point aggregation is so heavy that large aggregates are visually seen and tend to sediment to the bottom of the measuring vial. The carbohydrate decorated nanogels are clearly more stable than PNVCL-PA, but these nanogels are still not stable enough to withstand the high ionic concentrations of body fluids.

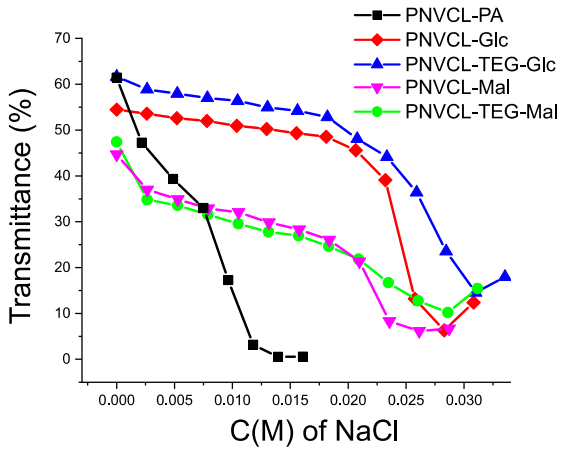

Figure 11 Salt induced aggregation test of PNVCL-PA and carbohydrate decorated PNVCL-PA nanogels

3.3.3.3 Availability of carbohydrates on the nanogels for binding

The availability of the carbohydrates on the nanogels was verified with an interaction study using a carbohydrate binding protein, Con A. Details of the experiment are described in paper III. As the carbohydrate decorated gels are thermoresponsive, it was of interest to study the temperature dependence of the Con A binding with one of the carbohydrate decorated PNVCL nanogels, PNVCL-TEG-Mal. Prior work on Con A binding to PNIPAm particles with carbohydrate groups randomly incorporated into the gel networks, have shown that the binding is dependent on the degree of gel swelling.[106,107] With the PNVCL-TEG-Mal particles, Con A was bound and precipitated as effectively at room temperature and at 37 °C (Figure 12 in paper II). The carbohydrates were available for interactions in both states of the nanogels, swollen and partly collapsed. The insensitivity to temperature is seen to be a result of the location of the carbohydrates on the outer parts of the nanogels.

3.3.4 PISA OF NVCL (PAPER III)

In polymerization induced self-assembly (PISA) reactions, the controlled chain extending of a solvophilic polymer with a solvophobic block results in a gradual self-assembly of the formed polymer into particles.[94] It is a potential method to synthesize soft nanoparticles, as high monomer concentrations can be used, no small surfactants are involved and the polymerization can yield interesting morphologies. The polymerization also yields block copolymers with predetermined molecular weights and narrow weight distributions. Thus, a fundamental study of emulsion polymerization induced self-assembly (PISA) of NVCL as the sole monomer was conducted.

The observations made on the nanogels produced with precipitation polymerization emphasized the importance of colloidal stabilization of the particles. For this reason, steric stabilization with a well-known non-ionic water soluble polymer PEG was of interest and it was used as the solvophilic block. The synthesis scheme is presented in Scheme 8.

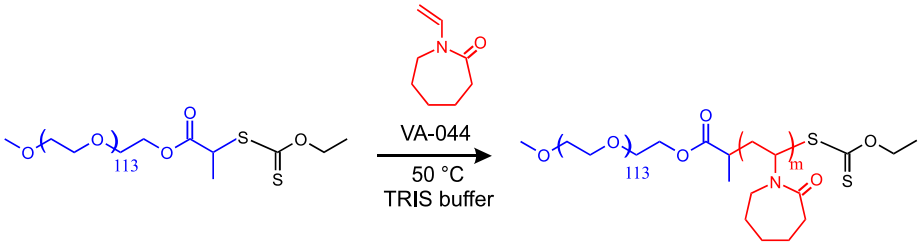

Scheme 8 PISA of NVCL

3.3.4.1 Preliminary tests and the effect of the PEG length

In preliminary experiments two different PEG lengths (DP = 42 or 113) were tested and only the polymerizations with the longer PEG (presented in scheme 8) produced stable dispersions. List of the polymerizations is presented in paper III.

With NVCL starting concentration 0.1 kg/l and higher the polymerization at 50 °C produced stable dispersions and the final monomer conversion was above 95% according to ^{1}H NMR. After purification with dialysis the product was obtained with high yield and was analyzed with SEC. Part of the reaction mixture was kept at 50 °C and analyzed with light scattering. Furthermore, a part of the hot mixture was diluted with saturated salicylic acid. Salicylic acid acts as a physical crosslinker by forming hydrogen bonds with NVCL and prevents the dissolution of the polymer upon cooling.

3.3.4.2 *Effect of the concentration*

PISA polymerizations were conducted with identical reagent ratios but with varying concentrations. Starting NVCL concentrations were 0.1 kg/l (10 wt% in respect to weight of buffer) 0.2 kg/l (20 wt% in respect to weight of buffer) and 0.3 kg/l (30 wt% in respect to weight of buffer). The concentrations are above the solubility limit of the monomer in TRIS buffer (0.036 kg/l at 50 °C, see paper III) and higher than concentrations usually used for the synthesis of PNVCL particles (0.1-3 wt%, see chapter 1.6). All the polymerizations performed with different solid contents produced stable dispersions. In addition to the increased reaction rate with increased concentration (see Figure 6, paper III), another more surprising effect was observed when studying the molecular weight of the purified products. The molar mass distribution became narrower when the solid content was increased (see Figure 12). In addition to the main product fraction in Figure 12, a lower molecular weight fraction was also observed. The fraction has similar size as the macroCTA used. Increasing the concentration made this fraction smaller.

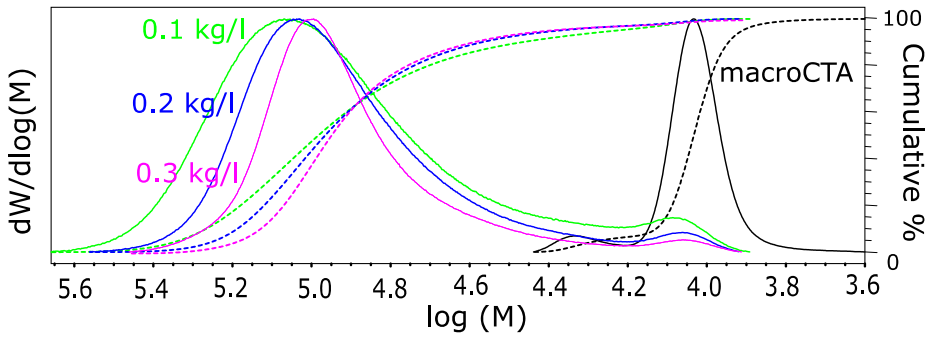

Figure 12 Molecular weight distributions obtained from SEC of PISA polymerizations with different concentrations. Starting NVCL concentration is given in the figure next to the respective solid curve. Dashed lines represent the cumulative mass% of the rescpective sample (same color). MacroCTA is shown as a reference.

3.3.4.3 *Effect of the PNVCL length*

By changing the ratio between NVCL and other reagents, the PNVCL length can be tailored. This was done to screen the capability of the reaction to produce particles with varying morphologies as the block ratio affects the shape of the self-assemblies. Theoretical M_n can be calculated based on the reagent ratio with equation 1. Reagent ratios, monomer : CTA : initiator ([M] : [CTA] : [I]) and M_n obtained with SEC are displayed in a table 3. As can be seen the measured M_n increased with increasing theoretical M_n, *i.e.* by changing the monomer to macroCTA ratio.

Table 3 *PISA polymertization of NVCL aiming at different PVCL lengths with starting concentration of NVCL being 0.1 kg/l*

[M] : [CTA] : [I]	Conversion	DP[a]	$M_{ntheory}$ [b]	M_{nSEC} [c]	$Đ_{SEC}$ (M_w/M_n) [c]
200/1/0.3	97	194	32 000	47 600	1.3
350/1/0.3	97	340	52 000	61 400	1.4
500/1/0.3	97	485	73 000	72 300	1.5
1000/1/0.3	98	980	141 000	122 000	1.3

a) DP = [M]/[CTA] × Conversion b) based on equation 1 c) SEC results based on the main peak in eluogram measured in THF with PMMA standadrs

Multi-angle light scattering measurements were performed on diluted samples of the reaction mixture at 50 °C to obtain data about the shape of the particles. The sample temperature was not allowed to change during the dilution. Light scattering was used to obtain both radius of gyration and the hydrodynamic radius. The ratio of the two can be used to estimate the shape of the scattering object. Model scatterers and the corresponding R_g/R_h values are presented in Scheme 9. By comparing the values in Scheme 9 with the values in Table 4, one can conclude that with increasing DP of PNVCL the polymer assemblies vary from thick walled vesicles (DP=194, R_g/R_h = 0.85) to spheres with slightly more compact cores than the shells (DP=980, R_g/R_h = 0.73)

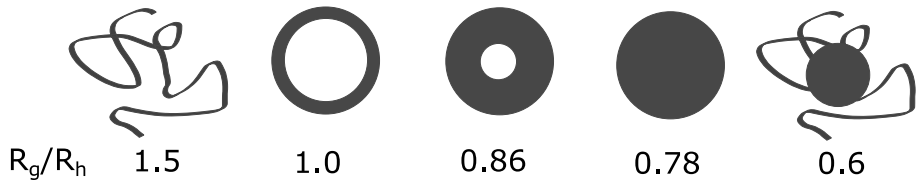

Scheme 9 R_g/R_h ratios and corresponding scatterers including; a random coil,[108] a thin walled vesicle,[109,110] a thick walled vesicle,[111] a homogenous sphere[108] and a sphere with denser core and loose shell[112,113].

Table 4 *Light scattering results for selected PISA products*

DP[a]	D_h [b] (nm)	R_g/R_h [b]	D_h [c] (nm)	R_g/R_h [c]
194	190	0.85	220	1.07
340	180	0.80	210	0.82
485	225	0.76	220	0.7
980	275	0.73	290	0.65

a) DP = [M]/[CTA] × conversion, b) diluted reaction mixture measured at 50 °C, c) Salicylic acid stabilized assemblies measured at 22 °C.

After physically crosslinking the assemblies with salicylic acid and cooling to 22 °C, the shape and size of the particles was measured again. The self-assemblies mostly maintained their size and shape with some exceptions. The salicylic acid stabilized assemblies were also imaged with cryo-TEM (Figure 13). The results support the conclusions made based on light scattering. For PNVCL with DP 194 and 340, vesicle type assemblies were seen in the cryo-TEM images as darker spheres with lighter cores. In the cryo-TEM images of the copolymer with PNVCL DP of 194, also other structures in addition to vesicles were seen, see Figure 10 in paper III. The presence of the non-spherical objects is seen as the reason why R_g/R_h of the salicylic acid stabilized polymer sample with PNVCL DP of 194 increased from 0.85 to 1.07 upon cooling. This is the polymer with the shortest PNVCL chains. It is possible that the salicylic acid stabilization was not effective enough for the assembly to keep its structure upon cooling.

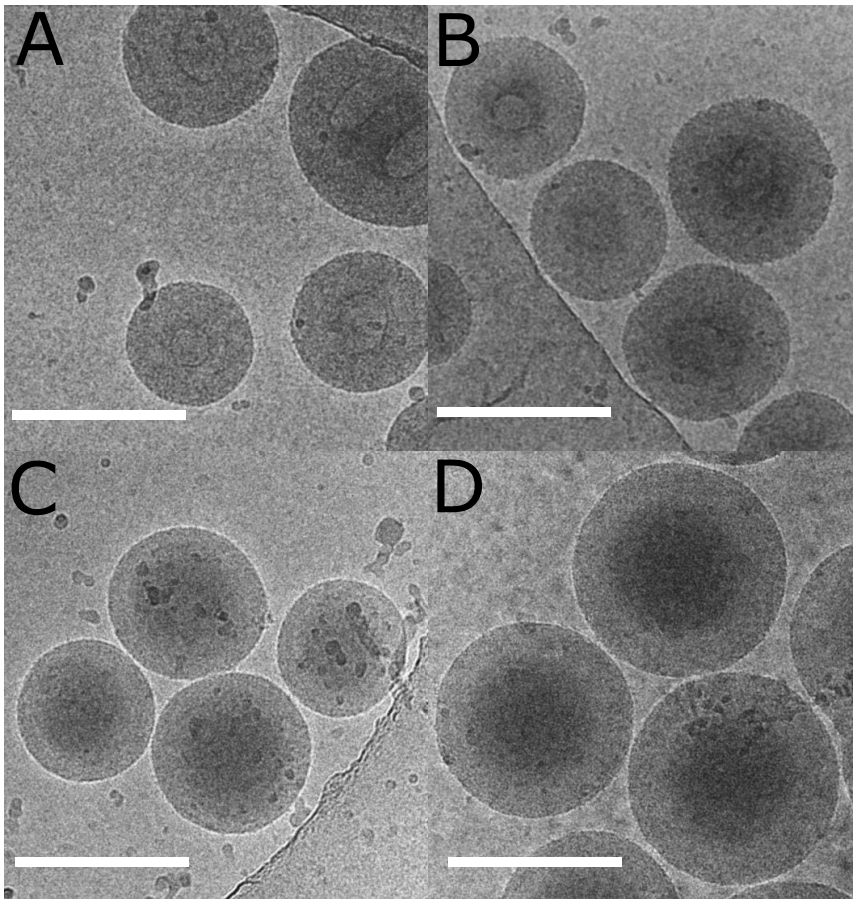

Figure 13 Cryogenic transmission electron microscopy images of the salicylic acid stabilized PNVCL assemblies presented in table 4. DP of the PNVCL block of the polymers is A) 194, B) 340, C) 485 and D) 980. The scale bar is 200 nm.

3.4 CONCLUSIONS

Soft PNVCL nanoparticles: crosslinked nanogels and self-assembled structures were studied. First, functionizable PNVCL nanogels were prepared with precipitation polymerization method using PA as a comonomer. PA was added after the formation of preparticles to obtain particles with propargyl functions in the shell. Incorporation of PA was successful and rendered the nanogels more compact. Based on conjugation reactions with an excess of carbohydrate azides, propargyl functions were proven to be available for functionalization using CuAAC and there were approximately 4 mol% of PA in respect to NVCL in the particles (6.7 mol% was used in the feed).

Propargyl functions on the nanogels were used for the decoration of the nanogels with gold nanoparticles. Gold nanoparticles rendered the nanogels responsive to blue light and to oscillating electric field. These particles have potential as multiresponsive carriers of active substances.

Functionalization of the propargyl functional nanogels with carbohydrate azides rendered the particles larger, more open, increased their size dispersity, and made the nanogels more stable against salt induced aggregation. The carbohydrates on the nanogels were proven to be available for binding with a protein, concanavalin A. Thus, targeting and interacting moieties can be incorporated to the propargyl functional nanogels via CuAAC.

As a final part of the dissertation, polymerization induced self-assembly (PISA) of NVCL as the sole monomer was studied. The effect of various reaction parameters was screened, and it was concluded that the method can be used to polymerize NVCL with higher solid content compared to the traditional precipitation polymerization method and with control over the molecular weight of the formed polymers. The particles, however, are not chemically crosslinked nanogels but instead self-assemblies that break to individual soluble block copolymer chains upon cooling. This can be prevented with physical crosslinking with salicylic acid, a molecule that forms crosslinking points between chains due to hydrogen bonding and hydrophobic interactions. The PISA approach is seen as a viable method for preparation soft PNVCL nanoparticles due to the level of control provided, no small surfactants needed, stability provided by the soluble block and due to the high concentrations.

4 REFERENCES

1. Vert, M.; Doi, Y.; Hellwich, K.; Hess, M.; Hodge, P.; Kubisa, P.; Rinaudo, M.; Schué, F. Terminology for biorelated polymers and applications (IUPAC Recommendations 2012). *Pure Appl. Chem.* **2012***, 84*, 377-410.

2. Pelaz, B.; Alexiou, C.; Alvarez-Puebla, R. A.; Alves, F.; Andrews, A. M.; Ashraf, S.; Balogh, L. P.; Ballerini, L.; Bestetti, A.; Brendel, C.; Bosi, S.; Carril, M.; Chan, W. C. W.; Chen, C.; Chen, X.; Chen, X.; Cheng, Z.; Cui, D.; Du, J.; Dullin, C.; Escudero, A.; Feliu, N.; Gao, M.; George, M.; Gogotsi, Y.; Grünweller, A.; Gu, Z.; Halas, N. J.; Hampp, N.; Hartmann, R. K.; Hersam, M. C.; Hunziker, P.; Jian, J.; Jiang, X.; Jungebluth, P.; Kadhiresan, P.; Kataoka, K.; Khademhosseini, A.; Kopeček, J.; Kotov, N. A.; Krug, H. F.; Lee, D. S.; Lehr, C.; Leong, K. W.; Liang, X.; Ling Lim, M.; Liz-Marzán, L. M.; Ma, X.; Macchiarini, P.; Meng, H.; Möhwald, H.; Mulvaney, P.; Nel, A. E.; Nie, S.; Nordlander, P.; Okano, T.; Oliveira, J.; Park, T. H.; Penner, R. M.; Prato, M.; Puntes, V.; Rotello, V. M.; Samarakoon, A.; Schaak, R. E.; Shen, Y.; Sjöqvist, S.; Skirtach, A. G.; Soliman, M. G.; Stevens, M. M.; Sung, H.; Tang, B. Z.; Tietze, R.; Udugama, B. N.; VanEpps, J. S.; Weil, T.; Weiss, P. S.; Willner, I.; Wu, Y.; Yang, L.; Yue, Z.; Zhang, Q.; Zhang, Q.; Zhang, X.; Zhao, Y.; Zhou, X.; Parak, W. J. Diverse Applications of Nanomedicine. *ACS Nano* **2017***, 11*, 2313-2381.

3. Estelrich J.; Quesada-Pérez M.; Forcada J.; Callejas-Fernández J. Introductory Aspects of Soft Nanoparticles, in *Soft nanoparticles for biomedical applications,* Edited by Callejas-Fernández, J.; Estelrich, J.; Quesada-Pérez, M.; Forcada, J. Royal Society of Chemistry; 2014

4. Alemán, J. V.; Chadwick, A. V.; He, J.; Hess, M.; Horie, K.; Jones, R. G.; Kratochvíl, P.; Meisel, I.; Mita, I.; Moad, G.; Penczek, S.; Stepto, R. F. T. Definitions of terms relating to the structure and processing of sols, gels, networks, and inorganic-organic hybrid materials (IUPAC Recommendations 2007). *Pure Appl. Chem.* **2007***, 79*, 1801-1829.

5. Plamper, F. A.; Richtering, W. Functional Microgels and Microgel Systems. *Acc. Chem. Res.* **2017***, 50*, 131-140.

6. Karg, M.; Pich, A.; Hellweg, T.; Hoare, T.; Lyon, L. A.; Crassous, J. J.; Suzuki, D.; Gumerov, R. A.; Schneider, S.; Potemkin, I. I.; Richtering, W. Nanogels and microgels: From model colloids to applications, recent developments and future trends. *Langmuir* **2019***, 35*, 6231-6255.

7. Brugger, B.; Vermant, J.; Richtering, W. Interfacial layers of stimuli-responsive poly-(*N*-isopropylacrylamide-co-methacrylicacid) (PNIPAM-co-MAA) microgels characterized by interfacial rheology and compression isotherms. *Phys. Chem. Chem. Phys.* **2010***, 12*, 14573-14578.

8. Fennel Evans, D.; Wennerstöm, H. *The colloidal domain : where physics, chemistry, biology, and technology meet,* 2nd edition*,* Wiley-VCH*,* 1999.

9. Owen, S. C.; Chan, D. P. Y.; Shoichet, M. S. Polymeric micelle stability. *Nano Today* **2012***, 7*, 53-65.

10. Aseyev, V.; Hietala, S.; Laukkanen, A.; Nuopponen, M.; Confortini, O.; Du Prez, F. E.; Tenhu, H. Mesoglobules of thermoresponsive polymers in dilute aqueous solutions above the LCST. *Polymer* **2005***, 46*, 7118-7131.

11. Shifrina, Z. B.; Matveeva, V. G.; Bronstein, L. M. Role of Polymer Structures in Catalysis by Transition Metal and Metal Oxide Nanoparticle Composites. *Chem. Rev.* **2020***, 120*, 1350-1396.

12. Zhang, Y.; Zhang, H.; Liu, P.; Sun, H.; Li, B.; Wang, W. Programming Hydrogen Production via Controllable Emulsification/Demulsification in a Switchable Oil–Water System. *ACS Sustainable Chem. Eng.* **2019***, 7*, 7768-7776.

13. Rosenblum, D.; Joshi, N.; Tao, W.; Karp, J. M.; Peer, D. Progress and challenges towards targeted delivery of cancer therapeutics. *Nat. Commun.* **2018***, 9*, 1410.

14. Matsumura, Y.; Maeda, H. A New Concept for Macromolecular Therapeutics in Cancer Chemotherapy: Mechanism of Tumoritropic Accumulation of Proteins and the Antitumor Agent Smancs. *Cancer Res.* **1986***, 46*, 6387.

15. Shi, J.; Kantoff, P. W.; Wooster, R.; Farokhzad, O. C. Cancer nanomedicine: progress, challenges and opportunities. *Nat. Rev. Cancer* **2016***, 17*, 20.

16. Wilhelm, S.; Tavares, A. J.; Dai, Q.; Ohta, S.; Audet, J.; Dvorak, H. F.; Chan, W. C. W. Analysis of nanoparticle delivery to tumours. *Nat. Rev. Mater.* **2016***, 1*, 16014.

17. Alkilany, A. M.; Zhu, L.; Weller, H.; Mews, A.; Parak, W. J.; Barz, M.; Feliu, N. Ligand density on nanoparticles: A parameter with critical impact on nanomedicine. *Adv. Drug Delivery Rev.* **2019***, 143*, 22-36.

18. Hui, Y.; Yi, X.; Hou, F.; Wibowo, D.; Zhang, F.; Zhao, D.; Gao, H.; Zhao, C. Role of Nanoparticle Mechanical Properties in Cancer Drug Delivery. *ACS Nano* **2019***, 13*, 7410-7424.

19. Anselmo, A. C.; Zhang, M.; Kumar, S.; Vogus, D. R.; Menegatti, S.; Helgeson, M. E.; Mitragotri, S. Elasticity of Nanoparticles Influences Their Blood Circulation, Phagocytosis, Endocytosis, and Targeting. *ACS Nano* **2015***, 9*, 3169-3177.

20. Zhang, L.; Cao, Z.; Li, Y.; Ella-Menye, J.; Bai, T.; Jiang, S. Softer Zwitterionic Nanogels for Longer Circulation and Lower Splenic Accumulation. *ACS Nano* **2012***, 6*, 6681-6686.

21. Hrubý, M.; Filippov, S. K.; Štěpánek, P. Smart polymers in drug delivery systems on crossroads: Which way deserves following? *Eur. Polym. J.* **2015***, 65*, 82-97.

22. Yang, D.; Viitasuo, M.; Pooch, F.; Tenhu, H.; Hietala, S. Poly(*N*-acryloylglycinamide) microgels as nanocatalyst platform. *Polym. Chem.* **2018***, 9*, 517-524.

23. Klinger, D.; Landfester, K. Stimuli-responsive microgels for the loading and release of functional compounds: Fundamental concepts and applications. *Polymer* **2012***, 53*, 5209-5231.

24. Cortez-Lemus, N. A.; Licea-Claverie, A. Poly(N-vinylcaprolactam), a comprehensive review on a thermoresponsive polymer becoming popular. *Prog. Polym. Sci.* **2016***, 53*, 1-51.

25. Kirsh, Y. E. *Water soluble poly-N-vinylamide : synthesis and physicochemical properties.* John Wiley & Sons, 1998.

26. Kirsh, Y. E.; Yanul, N. A.; Kalninsh, K. K. Structural transformations and water associate interactions in poly-*N*-vinylcaprolactam–water system. *Eur. Polym. J.* **1999***, 35*, 305-316.

27. Feldstein, M. M.; Bovaldinova, K. A.; Bermesheva, E. V.; Moscalets, A. P.; Dormidontova, E. E.; Grinberg, V. Y.; Khokhlov, A. R. Thermo-Switchable Pressure-Sensitive Adhesives Based on Poly(*N*-vinyl caprolactam) Non-Covalently Cross-Linked by Poly(ethylene glycol). *Macromolecules* **2014***, 47*, 5759-5767.

28. Kozlovskaya, V.; Baggett, J.; Godin, B.; Liu, X.; Kharlampieva, E. Hydrogen-Bonded Multilayers of Silk Fibroin: From Coatings to Cell-Mimicking Shaped Microcontainers. *ACS Macro Lett.* **2012***, 1*, 384-387.

29. Sefidroodi, H.; Cheng Chua, P.; Kelland, M. A. THF hydrate crystal growth inhibition with small anionic organic compounds and their synergistic properties with the kinetic hydrate inhibitor poly(N-vinylcaprolactam). *Chem. Eng. Sci.* **2011***, 66*, 2050-2056.

30. BASF Luviskol Plus. *https://www.carecreations.basf.com/product-formulations/products/products-detail/LUVISKOL%20PLUS/30054531* (accessed 29.11., 2019).

31. Vihola, H.; Laukkanen, A.; Valtola, L.; Tenhu, H.; Hirvonen, J. Cytotoxicity of thermosensitive polymers poly(*N*-isopropylacrylamide), poly(*N*-vinylcaprolactam) and amphiphilically modified poly(*N*-vinylcaprolactam). *Biomaterials* **2005***, 26*, 3055-3064.

32. BASF Soluplus. *https://pharmaceutical.basf.com/en/Drug-Formulation/Soluplus.html* (accessed 27.11.2019).

33. Meeussen, F.; Nies, E.; Berghmans, H.; Verbrugghe, S.; Goethals, E.; Du Prez, F. Phase behaviour of poly(*N*-vinyl caprolactam) in water. *Polymer* **2000***, 41*, 8597-8602.

34. Laukkanen, A.; Valtola, L.; Winnik, F. M.; Tenhu, H. Formation of Colloidally Stable Phase Separated Poly(*N*-vinylcaprolactam) in Water: A Study by Dynamic Light Scattering, Microcalorimetry, and Pressure Perturbation Calorimetry. *Macromolecules* **2004***, 37*, 2268-2274.

35. Sun, S.; Wu, P. Infrared Spectroscopic Insight into Hydration Behavior of Poly(*N*-vinylcaprolactam) in Water. *J. Phys. Chem. B.* **2011***, 115*, 11609-11618.

36. Spěváček, J.; Dybal, J.; Starovoytova, L.; Zhigunov, A.; Sedláková, Z. Temperature-induced phase separation and hydration in poly(*N*-vinylcaprolactam) aqueous solutions: a study by NMR and IR spectroscopy, SAXS, and quantum-chemical calculations. *Soft Matter* **2012***, 8*, 611-6119.

37. Sun, X.; Qian, X. Atomistic Molecular Dynamics Simulations of the Lower Critical Solution Temperature Transition of Poly(*N*-vinylcaprolactam) in Aqueous Solutions. *J. Phys. Chem. B* **2019***, 123*, 4986-4995.

38. Mikheeva, L. M.; Grinberg, N. V.; Mashkevich, A. Y.; Grinberg, V. Y.; Thanh, L. T. M.; Makhaeva, E. E.; Khokhlov, A. R. Microcalorimetric Study of Thermal Cooperative Transitions in Poly(*N*-vinylcaprolactam) Hydrogels. *Macromolecules* **1997***, 30*, 2693-2699.

39. Okur, H. I.; Hladílková, J.; Rembert, K. B.; Cho, Y.; Heyda, J.; Dzubiella, J.; Cremer, P. S.; Jungwirth, P. Beyond the Hofmeister Series: Ion-Specific Effects on Proteins and Their Biological Functions. *J. Phys. Chem. B.* **2017***, 121*, 1997-2014.

40. Moghaddam, S. Z.; Thormann, E. The Hofmeister series: Specific ion effects in aqueous polymer solutions. *J. Colloid Interface Sci.* **2019***, 555*, 615-635.

41. Maeda, Y.; Nakamura, T.; Ikeda, I. Hydration and Phase Behavior of Poly(*N*-vinylcaprolactam) and Poly(*N*-vinylpyrrolidone) in Water. *Macromolecules* **2002***, 35*, 217-222.

42. Strokov, I. V.; Abramchuk, S. S.; Makhaeva, E. E. Salt and pH effect on thermoresponsive behavior of multiwalled carbon nanotube (MWCNT)/poly(*N*-vinylcaprolactam) dispersion. *Colloid Polym. Sci.* **2019***, 297*, 387-395.

43. Liu, Z.; Wickramasinghe, S. R.; Qian, X. Ion-specificity in protein binding and recovery for the responsive hydrophobic poly(vinylcaprolactam) ligand. *RSC Advances* **2017***, 7*, 36351-3636.

44. Laukkanen, A.; Valtola, L.; Winnik, F. M.; Tenhu, H. Thermosensitive graft copolymers of an amphiphilic macromonomer and *N*-vinylcaprolactam:

synthesis and solution properties in dilute aqueous solutions below and above the LCST. *Polymer* **2005***, 46*, 7055-7065.

45. Kermagoret, A.; Fustin, C.; Bourguignon, M.; Detrembleur, C.; Jérôme, C.; Debuigne, A. One-pot controlled synthesis of double thermoresponsive N-vinylcaprolactam-based copolymers with tunable LCSTs. *Polym. Chem.* **2013***, 4*, 2575.

46. Jenkins, A. D.; Jones, R. G.; Moad, G. Terminology for reversible-deactivation radical polymerization previously called "controlled" radical or "living" radical polymerization (IUPAC Recommendations 2010). *Pure Appl. Sci.* **2009***, 82*, 483-491.

47. Hurtgen, M.; Liu, J.; Debuigne, A.; Jérôme , C.; Detrembleur, C. Synthesis of thermo-responsive poly(*N*-vinylcaprolactam)-containing block copolymers by cobalt-mediated radical polymerization. *J. Polym. Sci. Part A* **2012***, 50*, 400-408.

48. Etchenausia, L.; Rodrigues, A. M.; Harrisson, S.; Deniau Lejeune, E.; Save, M. RAFT Copolymerization of Vinyl Acetate and N-Vinylcaprolactam: Kinetics, Control, Copolymer Composition, and Thermoresponsive Self-Assembly. *Macromolecules* **2016***, 49*, 6799-6809.

49. Shao, L.; Hu, M.; Chen, L.; Xu, L.; Bi, Y. RAFT polymerization of *N*-vinylcaprolactam and effects of the end group on the thermal response of poly(*N*-vinylcaprolactam). *React. Funct. Polym.* **2012***, 72*, 407-413.

50. Kozlovskaya, V.; Liu, F.; Xue, B.; Ahmad, F.; Alford, A.; Saeed, M.; Kharlampieva, E. Polyphenolic Polymersomes of Temperature-Sensitive Poly(*N*-vinylcaprolactam)-block-Poly(*N*-vinylpyrrolidone) for Anticancer Therapy. *Biomacromolecules* **2017***, 18*, 2552-2563.

51. Liu, J.; Detrembleur, C.; De Pauw-Gillet, M.; Mornet, S.; Duguet, E.; Jérôme, C. Gold nanorods coated with a thermo-responsive poly(ethylene glycol)-b-poly(N-vinylcaprolactam) corona as drug delivery systems for remotely near infrared-triggered release. *Polym. Chem.* **2014***, 5*, 799-813.

52. Jia, F.; Wang, S.; Zhang, X.; Xiao, C.; Tao, Y.; Wang, X. Amino-functionalized poly(*N*-vinylcaprolactam) derived from lysine: a sustainable polymer with thermo and pH dual stimuli response. *Polym. Chem.* **2016***, 7*, 7101-7107.

53. Cortez-Lemus N. A.; Licea-Claverie A. Preparation of a Mini-Library of Thermo-Responsive Star (NVCL/NVP-VAc) Polymers with Tailored Properties Using a Hexafunctional Xanthate RAFT Agent. *Polymers* **2018***, 10*, 20.

54. Zhao, X.; Coutelier, O.; Nguyen, H. H.; Delmas, C.; Destarac, M.; Marty, J. Effect of copolymer composition of RAFT/MADIX-derived *N*-vinylcaprolactam/*N*-vinylpyrrolidone statistical copolymers on their

thermoresponsive behavior and hydrogel properties. *Polym. Chem.* **2015***, 6*, 5233-5243.

55. Karesoja, M.; Karjalainen, E.; Hietala, S.; Tenhu, H. Phase Separation of Aqueous Poly(2-dimethylaminoethyl methacrylate-block-*N*-vinylcaprolactams). *J. Phys. Chem. B* **2014***, 118*, 10776-10784.

56. Beija, M.; Marty, J.; Destarac, M. Thermoresponsive poly(*N*-vinyl caprolactam)-coated gold nanoparticles: sharp reversible response and easy tunability. *Chem. Commun.* **2011***, 47*, 2826-2828.

57. Van Nieuwenhove, I.; Maji, S.; Dash, M.; Van Vlierberghe, S.; Hoogenboom, R.; Dubruel, P. RAFT/MADIX polymerization of *N*-vinylcaprolactam in water–ethanol solvent mixtures. *Polym. Chem.* **2017***, 8*, 2433-2437.

58. Pooja, S.; Ambika, S.; Rajesh, K. Synthesis of amphiphilic poly(*N*-vinylcaprolactam) using ATRP protocol and antibacterial study of its silver nanocomposite. *J. Polym. Sci. A Polym. Chem.* **2012***, 50*, 1503-1514.

59. Jiang, X.; Li, Y.; Lu, G.; Huang, X. A novel poly(*N*-vinylcaprolactam)-based well-defined amphiphilic graft copolymer synthesized by successive RAFT and ATRP. *Polym. Chem.* **2013***, 4*, 1402-1411.

60. Moad, G.; Barner-Kowollik, C. In *Handbook of RAFT Polymerization.* Edited by Barner-Kowollik, C. Wiley-VCH, 2008.

61. Perrier, S. 50th Anniversary Perspective: RAFT Polymerization - A User Guide. *Macromolecules* **2017***, 50*, 7433-7447.

62. Vihola, H.; Laukkanen, A.; Tenhu, H.; Hirvonen, J. Drug release characteristics of physically cross-linked thermosensitive poly(*N*-vinylcaprolactam) hydrogel particles. *J. Pharm. Sci.* **2008***, 97*, 4783-4793.

63. Kozlovskaya, V.; Liu, F.; Xue, B.; Ahmad, F.; Alford, A.; Saeed, M.; Kharlampieva, E. Polyphenolic Polymersomes of Temperature-Sensitive Poly(N-vinylcaprolactam)-block-Poly(N-vinylpyrrolidone) for Anticancer Therapy. *Biomacromolecules* **2017***, 18*, 2552-2563.

64. Mani, P.; Grailer, J. J.; Steeber, D. A.; Shaoqin, G. Thermosensitive Micelles Based on Folate-Conjugated Poly(N-vinylcaprolactam)-block-Poly(ethylene glycol) for Tumor-Targeted Drug Delivery. *Macromol. Biosci.* **2009***, 9*, 744-753.

65. Liu, F.; Kozlovskaya, V.; Medipelli, S.; Xue, B.; Ahmad, F.; Saeed, M.; Cropek, D.; Kharlampieva, E. Temperature-Sensitive Polymersomes for Controlled Delivery of Anticancer Drugs. *Chem. Mater.* **2015***, 27*, 7945-7956.

66. Kozlovskaya, V.; Kharlampieva, E. Self-Assemblies of Thermoresponsive Poly(N-vinylcaprolactam) Polymers for Applications in Biomedical Field. *ACS Appl. Polym. Mater.* **2020***, 2*, 26-39.

67. Laukkanen, A.; Hietala, S.; Maunu, S. L.; Tenhu, H. Poly(*N*-vinylcaprolactam) Microgel Particles Grafted with Amphiphilic Chains. *Macromolecules* **2000***, 33*, 8703-8708.

68. Laukkanen, A.; Wiedmer, S. K.; Varjo, S.; Riekkola, M.; Tenhu, H. Stability and thermosensitive properties of various poly (*N*-vinylcaprolactam) microgels. *Colloid Polym. Sci.* **2002***, 280*, 65-70.

69. Vihola, H.; Laukkanen, A.; Hirvonen, J.; Tenhu, H. Binding and release of drugs into and from thermosensitive poly(*N*-vinyl caprolactam) nanoparticles. *Eur. J. Pharm. Sci.* **2002***, 16*, 69-74.

70. Häntzschel, N.; Zhang, F.; Eckert, F.; Pich, A.; Winnik, M. A. Poly(*N*-vinylcaprolactam-co-glycidyl methacrylate) Aqueous Microgels Labeled with Fluorescent LaF3:Eu Nanoparticles. *Langmuir* **2007***, 23*, 10793-10800.

71. Imaz, A.; Forcada, J. *N*-vinylcaprolactam-based microgels: Synthesis and characterization. *J. Polym. Sci. A Polym. Chem.* **2008***, 46*, 2510-2524.

72. Imaz, A.; Forcada, J. *N*-vinylcaprolactam-based microgels: Effect of the concentration and type of cross-linker. *J. Polym. Sci. A Polym. Chem.* **2008***, 46*, 2766-2775.

73. Imaz, A.; Forcada, J. Optimized buffered polymerizations to produce *N*-vinylcaprolactam-based microgels. *Eur. Polym. J.* **2009***, 45*, 3164-3175.

74. Pich, A.; Berger, S.; Ornatsky, O.; Baranov, V.; Winnik, M. A. The influence of PEG macromonomers on the size and properties of thermosensitive aqueous microgels. *Colloid Polym. Sci.* **2009***, 287*, 269-275.

75. Imaz, A.; Forcada, J. Synthesis strategies to incorporate acrylic acid into *N*-vinylcaprolactam-based microgels. *J. Polym. Sci. A Polym. Chem.* **2011***, 49*, 3218-3227.

76. Wang, Y.; Nie, J.; Chang, B.; Sun, Y.; Yang, W. Poly(vinylcaprolactam)-Based Biodegradable Multiresponsive Microgels for Drug Delivery. *Biomacromolecules* **2013***, 14*, 3034-3046.

77. Schneider, F.; Balaceanu, A.; Feoktystov, A.; Pipich, V.; Wu, Y.; Allgaier, J.; Pyckhout-Hintzen, W.; Pich, A.; Schneider, G. J. Monitoring the Internal Structure of Poly(*N*-vinylcaprolactam) Microgels with Variable Cross-Link Concentration. *Langmuir* **2014***, 30*, 15317-15326.

78. Lou, S.; Gao, S.; Wang, W.; Zhang, M.; Zhang, Q.; Wang, C.; Li, C.; Kong, D. Temperature/pH dual responsive microgels of crosslinked poly(*N*-

vinylcaprolactam-co-undecenoic acid) as biocompatible materials for controlled release of doxorubicin. *J. Appl. Polym. Sci.* **2014***, 131*, 41146,

79. Gonzalez-Ayon, M. A.; Cortez-Lemus, N. A.; Zizumbo-Lopez, A.; Licea-Claverie, A. Nanogels of Poly(*N*-Vinylcaprolactam) Core and Polyethyleneglycol Shell by Surfactant Free Emulsion Polymerization. *Soft Mater.* **2014***, 12*, 315-325.

80. González-Ayón, M. A.; Sañudo-Barajas, J. A.; Picos-Corrales, L. A.; Licea-Claverie, A. PNVCL-PEGMA nanohydrogels with tailored transition temperature for controlled delivery of 5-fluorouracil. *J. Polym. Sci. Part A: Polym. Chem.* **2015***, 53*, 2662-2672.

81. Gau, E.; Mate, D. M.; Zou, Z.; Oppermann, A.; Töpel, A.; Jakob, F.; Wöll, D.; Schwaneberg, U.; Pich, A. Sortase-Mediated Surface Functionalization of Stimuli-Responsive Microgels. *Biomacromolecules* **2017***, 18*, 2789-2798.

82. Willems, C.; Pargen, S.; Balaceanu, A.; Keul, H.; Möller, M.; Pich, A. Stimuli responsive microgels decorated with oligoglycidol macromonomers: Synthesis, characterization and properties in aqueous solution. *Polymer* **2018***, 141*, 21-33.

83. Macchione, M. A.; Guerrero-Beltrán, C.; Rosso, A. P.; Euti, E. M.; Martinelli, M.; Strumia, M. C.; Muñoz-Fernández, M. Á Poly(*N*-vinylcaprolactam) Nanogels with Antiviral Behavior against HIV-1 Infection. *Sci. Rep.* **2019***, 9*, 5732-10.

84. Bian, S.; Zheng, J.; Tang, X.; Yi, D.; Wang, Y.; Yang, W. One-Pot Synthesis of Redox-Labile Polymer Capsules via Emulsion Droplet-Mediated Precipitation Polymerization. *Chem. Mater.* **2015***, 27*, 1262-1268.

85. Stanislaw, S.; Alemán José, V.; Gilbert Robert, G.; Michael, H.; Kazuyuki, H.; Jones Richard, G.; Przemyslaw, K.; Ingrid, M.; Werner, M.; Penczek Stanisław; Stepto Robert, F. T. Terminology of polymers and polymerization processes in dispersed systems (IUPAC Recommendations 2011). *Pure Appl. Chem.* **2011***, 83*, 2229.

86. Crespy, D.; Zuber, S.; Turshatov, A.; Landfester, K.; Popa, A. A straightforward synthesis of fluorescent and temperature-responsive nanogels. *J. Polym. Sci. A Polym. Chem.* **2012***, 50*, 1043-1048.

87. Petrizza, L.; Le Bechec, M.; Decompte, E.; El Hadri, H.; Lacombe, S.; Save, M. Tuning photosensitized singlet oxygen production from microgels synthesized by polymerization in aqueous dispersed media. *Polym. Chem.* **2019***, 10*, 3170-3179.

88. Medeiros, S. F.; Santos, A. M.; Fessi, H.; Elaissari, A. Synthesis of biocompatible and thermally sensitive poly(*N*-vinylcaprolactam) nanogels via inverse miniemulsion polymerization: Effect of the surfactant concentration. *J. Polym. Sci. A Polym. Chem.* **2010***, 48*, 3932-3941.

89. Gao, F.; Mi, Y.; Wu, X.; Yao, J.; Qi, Q.; Cao, Z. Preparation of thermoresponsive poly(*N*-vinylcaprolactam-co-2-methoxyethyl acrylate) nanogels via inverse miniemulsion polymerization. *J. Appl. Polym. Sci.* **2019***, 136*, 48237.

90. Schork, F.; Luo, Y.; Smulders, W.; Russum, J.; Butté, A.; Fontenot, K. Miniemulsion Polymerization, in *Polymer Particles*, Edited by Okubo, M. Springer, 2005; Vol. 175, pp 129-255.

91. Landfester, K. Miniemulsion Polymerization and the Structure of Polymer and Hybrid Nanoparticles. *Angew. Chem., Int. Ed.* **2009***, 48*, 4488-4507.

92. Gumerov, R. A.; Gau, E.; Xu, W.; Melle, A.; Filippov, S. A.; Sorokina, A. S.; Wolter, N. A.; Pich, A.; Potemkin, I. I. Amphiphilic PVCL/TBCHA microgels: From synthesis to characterization in a highly selective solvent. *J. Colloid Interface Sci.* **2020***, 564*, 344-356.

93. Kehren, D.; Lopez, C. M.; Theiler, S.; Keul, H.; Möller, M.; Pich, A. Multicompartment aqueous microgels with degradable hydrophobic domains. *Polymer* **2019***, 172*, 283-293.

94. Canning, S. L.; Smith, G. N.; Armes, S. P. A Critical Appraisal of RAFT-Mediated Polymerization-Induced Self-Assembly. *Macromolecules* **2016***, 49*, 1985-2001.

95. Khor, S. Y.; Quinn, J. F.; Whittaker, M. R.; Truong, N. P.; Davis, T. P. Controlling Nanomaterial Size and Shape for Biomedical Applications via Polymerization-Induced Self-Assembly. *Macromol. Rapid Commun.* **2019***, 40*, 1800438.

96. Etchenausia, L.; Deniau, E.; Brûlet, A.; Forcada, J.; Save, M. Cationic Thermoresponsive Poly(*N*-vinylcaprolactam) Microgels Synthesized by Emulsion Polymerization Using a Reactive Cationic Macro-RAFT Agent. *Macromolecules* **2018***, 51*, 2551-2563.

97. Etchenausia, L.; Khoukh, A.; Deniau Lejeune, E.; Save, M. RAFT/MADIX emulsion copolymerization of vinyl acetate and *N*-vinylcaprolactam: towards waterborne physically crosslinked thermoresponsive particles. *Polym. Chem.* **2017***, 8*, 2244-2256.

98. Collins, C. B.; McCoy, R. S.; Ackerson, B. J.; Collins, G. J.; Ackerson, C. J. Radiofrequency heating pathways for gold nanoparticles. *Nanoscale* **2014***, 6*, 8459-8472.

99. Collins, C. B.; Tofanelli, M. A.; Noblitt, S. D.; Ackerson, C. J. Electrophoretic Mechanism of Au25(SR)18 Heating in Radiofrequency Fields. *J. Phys. Chem. Lett.* **2018***, 9*, 1516-1521.

100. Pantano, P.; Harrison, C. D.; Poulose, J.; Urrabazo, D.; Norman, T. Q.; Braun, E. I.; Draper, R. K.; Overzet, L. J. Factors affecting the 13.56-MHz radio-frequency-mediated heating of gold nanoparticles. *Appl. Spectrosc. Rev.* **2017**, 1-16.

101. Slavík, J. Anilinonaphthalene sulfonate as a probe of membrane composition and function. *Biochim. Biophys. Acta, Biomembr.* **1982***, 694*, 1-25.

102. Matulis, D.; Baumann, C. G.; Bloomfield, V. A.; Lovrien, R. E. 1-Anilino-8-naphthalene sulfonate as a protein conformational tightening agent. *Biopolymers* **1999***, 49*, 451-458.

103. Bondarev, S. L.; Knyukshto, V. N.; Stepuro, V. I.; Stupak, A. P.; Turban, A. A. Fluorescence and Electronic Structure of the Laser Dye DCM in Solutions and in Polymethylmethacrylate. *J. Appl. Spectorsc.* **2004***, 71*, 194-201.

104. Qin, Y.; Zhang, P.; Lai, L.; Tian, Z.; Zheng, S.; Lu, J. Luminous composite ultrathin films of the DCM dye assembled with layered double hydroxides and its fluorescence solvatochromism properties for polarity sensors. *J. Mater. Chem.* **2015***, 3*, 5246-5252.

105. Vatanparast, R.; Li, S.; Hakala, K.; Lemmetyinen, H. Monitoring of Curing of Polyurethane Polymers with Fluorescence Method. *Macromolecules* **2000***, 33*, 438-443.

106. Hoshino, Y.; Nakamoto, M.; Miura, Y. Control of Protein-Binding Kinetics on Synthetic Polymer Nanoparticles by Tuning Flexibility and Inducing Conformation Changes of Polymer Chains. *J. Am. Chem. Soc.* **2012***, 134*, 15209-15212.

107. Paul, T. J.; Rübel, S.; Hildebrandt, M.; Strzelczyk, A. K.; Spormann, C.; Lindhorst, T. K.; Schmidt, S. Thermosensitive Display of Carbohydrate Ligands on Microgels for Switchable Binding of Proteins and Bacteria. *ACS Appl. Mater. Interfaces* **2019***, 11*, 26674-26683.

108. Schärtl, W. *Light scattering from polymer solutions and nanoparticle dispersions,* Springer: 2007.

109 Abdelmohsen, L. K. E. A; Rikken, R. S. M.; Christianen, P. C. M.; van Hest, J. C. M.; Wilson, D. A. Shape characterization of polymersome morphologies via light scattering techniques. *Polymer* **2016***, 107*, 445-449.

110. Constable, E.,C.; Mundwiler, S.; Meier, W.; Nardin, C. Reversible metal-directed assembly of clusters of vesicles. *Chem. Commun.* **1999**, 1483-1484.

111. Dou, H.; Jiang, M.; Peng, H.; Chen, D.; Hong, Y. pH-Dependent Self-Assembly: Micellization and Micelle–Hollow-Sphere Transition of Cellulose-Based Copolymers. *Angew. Chem., Int. Ed.* **2003***, 42*, 1516-1519.

112. Senff, H.; Richtering, W. Influence of cross-link density on rheological properties of temperature-sensitive microgel suspensions. *Colloid Polym. Sci.* **2000***, 278*, 830-840.

113. Boyko, V.; Pich, A.; Lu, Y.; Richter, S.; Arndt, K.; Adler, H. P. Thermo-sensitive poly(*N*-vinylcaprolactam-co-acetoacetoxyethyl methacrylate) microgels: 1—synthesis and characterization. *Polymer* **2003***, 44*, 7821-7827.